
Towards Explanation for Unsupervised Graph-Level Representation Learning

Qinghua Zheng¹ Jihong Wang¹ Minnan Luo¹ Yaoliang Yu² Jundong Li³

Lina Yao⁴ Xiaojun Chang⁵

¹Xi'an Jiaotong University

²University of Waterloo

³University of Virginia

⁴University of New South Wales

⁵University of Technology Sydney

qhzheng@xjtu.edu.cn, wang1946456505@stu.xjtu.edu.cn, minnluo@xjtu.edu.cn

yaoliang.yu@uwaterloo.ca, jundong@virginia.edu, lina.yao@unsw.edu.au

xiaojun.chang@uts.edu.au

Abstract

Due to the superior performance of Graph Neural Networks (GNNs) in various domains, there is an increasing interest in the GNN explanation problem "*which fraction of the input graph is the most crucial to decide the model's decision?*" Existing explanation methods focus on the supervised settings, *e.g.*, node classification and graph classification, while the explanation for unsupervised graph-level representation learning is still unexplored. The opaqueness of the graph representations may lead to unexpected risks when deployed for high-stake decision-making scenarios. In this paper, we advance the Information Bottleneck principle (IB) to tackle the proposed explanation problem for unsupervised graph representations, which leads to a novel principle, *Unsupervised Subgraph Information Bottleneck* (USIB). We also theoretically analyze the connection between graph representations and explanatory subgraphs on the label space, which reveals that the expressiveness and robustness of representations benefit the fidelity of explanatory subgraphs. Experimental results on both synthetic and real-world datasets demonstrate the superiority of our developed explainer and the validity of our theoretical analysis.

1 Introduction

Graph Neural Networks (GNNs) have emerged as a promising learning paradigm and demonstrated superior learning performance on different graph learning tasks, such as node classification [1, 2, 3, 4], graph classification [5, 6], and link prediction [7, 8]. Despite their strengths, GNNs are usually treated as black boxes and thus cannot provide human-intelligible explanations [9, 10]. Such opaqueness impedes their broad adoption in many decision-critical applications pertaining to fairness, privacy, and safety [11]. To better understand the working mechanisms of GNNs, researchers focus on the GNN explanation problem recently: *what knowledge does the GNN model extract to make the specific decision?* Specifically, given a graph and a GNN model, explanation methods try to find the intrinsic graph components that are crucial in the procedure of prediction for the target instance. To the best of our knowledge, all existing works [12, 13, 9, 14] only consider explanations in supervised settings, such as graph classification and node classification. More specifically, these works aim to provide trusty explanations on why graphs and nodes are classified into a specific category by GNN models. However, the explanation problem for unsupervised graph representation learning is still unexplored. Different from supervised GNNs, unsupervised graph representation learning methods [15, 16, 17, 18] embed graph data into low-dimensional representations without any supervision

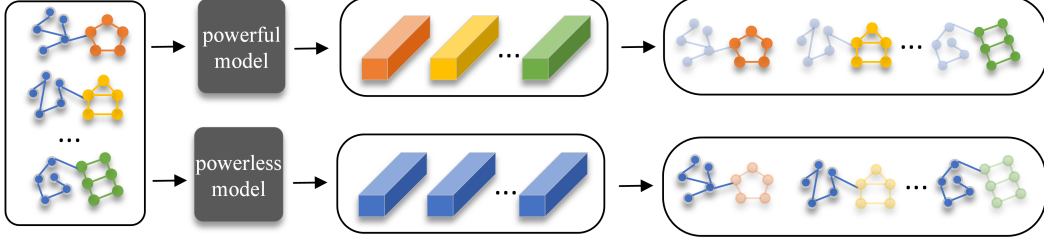


Figure 1: An intuition of explanation for unsupervised graph representation. Given graphs with different motifs (*i.e.*, cycle, house and grid), expressive and robust representations generated by powerful GNNs can exactly extract the motif-related information and ignore the random noises. Thus explanatory subgraphs for the powerful representations can explore the essential structure and vice versa.

signals. Because of their opaqueness, it is hazardous to employ these representations for high-stake decision-making problems directly. In consequence, it is imperative to lift the veil of unsupervised graph representations by answering the following question: *what knowledge do unsupervised GNNs incorporate to generate the graph representations?*

To provide a universal perspective, in this paper, we focus on the explanation for unsupervised graph-level representations¹. Specifically, we aim to find explanatory subgraphs most relevant to the representations while incorporating superfluous information as little as possible. There are mainly two challenges in the unexplored explanation problem: (1) Different from supervised GNNs which are designed for specific tasks, unsupervised graph representations are usually task-agnostic. Thus, existing explanation methods based on specific learning tasks cannot be directly grafted to explain unsupervised graph representations. (2) It is computational intractably to evaluate the relevance between the subgraphs and the representation vectors since they are located in different spaces, *i.e.*, the non-Euclidean space and Euclidean space, respectively. As a result, an effective and efficient measurement is urgently needed.

To address the above challenges, we propose a novel method named *Unsupervised Subgraph Information Bottleneck* (USIB) in light of the Information Bottleneck (IB) principle [19, 20] that learns compressed representations from the input data while keeping the most predictive information of labels. Specifically, USIB adopts the mutual information to formalize the relevance. It maximizes the mutual information between explanatory subgraphs and graph representations while minimizing the mutual information between explanatory subgraphs and given graph instances, simultaneously. Moreover, we theoretically analyze the connection between representations and explanatory subgraphs on the label space, which reveals that the expressiveness and robustness of representations benefit the fidelity of explanatory subgraphs. Intuitively, as shown in Fig. 1, when the graphs have different motifs, expressive and robust representations extract the motif-related information exactly while uninformative and fragile representations focus more on noises. Thus, explanations generated for powerful representations can explore the essential structure, while the fidelity of explanation for powerless representations is not guaranteed. The contributions of this paper are summarized as follows.

- We consider an unexplored explanation problem. To the best of our knowledge, this is the first work to explore the explanation for unsupervised graph representation learning with GNNs.
- We propose a novel explanation method USIB based on the IB principle, which aims to find the most informative yet compressed explanation. We also theoretically analyze the connection between representations and explanatory subgraphs on the label space, revealing that representations' expressiveness and robustness benefit the explanatory subgraphs.
- Extensive experiments show that our method achieves the state-of-the-art performance on several benchmark datasets and also demonstrate the validity of our theoretical analysis.

¹The explanation for node-level representations can be seen as a particular case by considering the corresponding k -hop neighbor subgraphs of each node as a graph instance.

2 Related works

Instance-level explanation. Instance-level explanation aims to give explanations for specific instances. In general, there are mainly two lines of works: (1) Non-parametric explanation methods [21, 12, 22, 23] usually involve gradient-like scores as heuristics to quantify the importance of edges and nodes. The gradient-like scores can be easily obtained by conducting backpropagation from the target model prediction to the input, *e.g.*, adjacency matrix. For example, SA [21] directly employs the squared values of gradients as the importance scores of different input features. However, these methods can only reflect the sensitivity between input and output, which cannot accurately show the importance. (2) Parametric explanation methods [9, 24, 10, 25, 14] generate the explanatory subgraphs with a parametrized explainer model. To name a few, GNNExplainer [9] learns soft masks with a local view and applies the masks on the adjacency matrix. To provide a global understanding of the model prediction, PGExplainer [10] generates the explanatory subgraphs with a deep neural network whose parameters are shared across the explained instances. Moreover, to simultaneously exhibit the local and global explainability, Refine [25] adopts the pre-training and fine-tuning techniques to explain GNNs.

Model-level explanation. Model-level explanation aims to provide general insights and high-level understanding to explain deep graph models. The only existing model-level method for explaining graph neural networks is XGNN [26] that explains GNNs by training a graph generator, so as to output class-wise graph patterns to explain a specific class. However, to our best knowledge, all existing explanation methods focus on end-to-end GNNs in the framework of supervised learning, *e.g.*, node classification and graph classification GNN models are mostly studied. In this regard, it is still unexplored how to make explanations for unsupervised graph representation learning.

3 Notations and preliminaries

Notations. In most cases, we denote random variables with upper-case letters (*e.g.*, G and Z), and represent its support set by calligraphic letters (*e.g.*, \mathcal{G} and \mathcal{Z}). Upper-case letters with superscript (*e.g.*, $G^{(k)}$ and $Z^{(m)}$) refers to the instances of random variables correspondingly. Suppose the graph data is given as $G = (\mathcal{V}, \mathcal{E})$, where \mathcal{V} and \mathcal{E} are the nodes and edges respectively. The representations of graph G , denoted as Z , is learned by an unsupervised GNN model $f_t : \mathcal{G} \rightarrow \mathcal{Z}$, such as the state-of-the-arts Infograph[27], GCL [28], and ADGCL [29]. Moreover, we denote the ground-truth labels of graphs as Y which are unreachable in the unsupervised setting.

Information Bottleneck [30, 31]. Given input data X and its label Y , Information Bottleneck aims to discover a compressed latent representation Z that is maximally informative in terms of Y . Formally, one can learn the latent representation Z by optimizing the following optimization problem

$$\max_Z \mathcal{L}_{IB} = I(Z; Y) - \beta I(X; Z) \quad (1)$$

where β denotes a hyper-parameter trading-off the informativeness and compression. Mutual information (MI) $I(X; Z)$ measures the relevance of two random variables, formulated as $I(X; Z) = \int_x \int_z p(x, z) \log \frac{p(x, z)}{p(x)p(z)} dx dz$.

GNN explanation. GNN explanation aims to understand the intrinsic information of the graphs that are crucial for GNN’s computation process, so as to provide human-intelligible explanations. Specifically, given a graph G and a GNN model ψ that learns a conditional distribution $P_\psi(\hat{Z}|G)$, GNN explanation aims to learn explanatory subgraphs S that are most relevant with GNN’s computation results, *i.e.*,

$$S = \arg \max_{S \in \mathcal{S}} Score(S, \hat{Z}) \quad (2)$$

where \mathcal{S} denotes the universe set consisting of all possible subgraphs of graph G ; $Score(S, \hat{Z})$ measures the relevance between subgraph S and GNN’s computation results \hat{Z} . For example, GNNExplainer [9] focuses on the explanation for supervised GNNs, and formalizes the relevance $Score(S, \hat{Z})$ as mutual information, *i.e.*, $S = \arg \max_{S \in \mathcal{S}} I(S; \hat{Y})$, where random variable $\hat{Y} = \hat{Z}$ refers to the classification probabilities.

4 Methodology

In this section, we first introduce our proposed explanation method for unsupervised graph representation learning, *i.e.*, USIB. Then, we elaborate on the mutual information estimation methods for USIB. Finally, the reparameterization trick is presented for the optimization of USIB objective.

4.1 Unsupervised Subgraph Information Bottleneck

In this paper, we study the unexplored explanation problem for unsupervised graph-level representation learning. Given a graph G and its corresponding representation Z extracted by unsupervised GNNs, our goal is to identify the explanatory subgraph S that is most relevant to the representations. Following the previous explanation works [9, 10], we leverage mutual information to measure the relevance and therefore formulate the explanation problem as $\arg \max_S I(S; Z)$. Unfortunately, it has been proved that there is a trivial solution $S = G$ since $I(Z; S) \leq I(Z; G)$ (The proof is shown in the Appendix B). The trivial solution indicates that the explanatory subgraph S may incorporate superfluous information, *e.g.*, noise and irrelevant information with representations Z . Inspired by the success of IB principle in explanation for supervised GNNs [19], we generalize the IB principle to the unsupervised setting to avoid the trivial solution and exploit a novel principle.

Definition. (*Unsupervised Subgraph Information Bottleneck: USIB*). *Given a graph G and its representation Z , the USIB seeks for the most informative yet compressed explanation S through optimization problem*

$$\max_S \mathcal{L}_{USIB} = I(Z; S) - \beta I(G; S). \quad (3)$$

By optimizing the USIB objective, one can make a trade-off between the informativeness and compression of explanatory subgraphs. However, it is notoriously intractable to optimize the USIB objective because the mutual information involves integral on high-dimensional data, *i.e.*, Z , S , and G . As a result, a mutual information estimation method is necessary to be exploited.

4.2 Optimization for USIB

We tackle the two terms $I(Z; S)$ and $I(G; S)$ in the objective of USIB separately.

Maximizing $I(Z; S)$. We adopt Jensen-Shannon MI estimator [32, 33] to assign an approximate lower bound for $I(Z; S)$, *i.e.*,

$$\hat{I}^{JSD}(Z; S) := \sup_{f_\phi} \mathbb{E}_{p(S, Z)} [-sp(-f_\phi(S, Z))] - \mathbb{E}_{p(S), p(Z)} [sp(f_\phi(S, Z))] \quad (4)$$

where $sp(x) = \log(1 + e^x)$ is the softplus function; Function $f_\phi : \mathcal{S} \times \mathcal{Z} \rightarrow \mathbb{R}$ with parameters ϕ is learned to discriminate whether an instance of S and an instance of Z are sampled from the joint distribution or not. It is implemented with function composite of MLP_{ϕ_1} and GNN_{ϕ_2} , *i.e.*,

$$f_\phi(S^{(k)}, Z^{(k)}) = \text{MLP}_{\phi_1} \left(\text{GNN}_{\phi_2} \left(S^{(k)} \right) \| Z^{(k)} \right) \quad (5)$$

where $\phi = \{\phi_1, \phi_2\}$; $\|$ refers to the concatenation operator. Note that the prior distributions $p(S, Z)$ and $p(Z)$ are usually unreachable in practice. In conjunction with Monte Carlo sampling to approximate the prior distributions, we reach an approximate lower bound of Eq. (4) by

$$\max_{\phi} \mathcal{L}_1(\phi, S) = \frac{1}{K} \sum_{k=1}^K -sp \left(-f_\phi(S^{(k)}, Z^{(k)}) \right) - \frac{1}{K} \sum_{k=1, m \neq k}^K sp \left(f_\phi(S^{(k)}, Z^{(m)}) \right) \quad (6)$$

where K is the number of samples. $(S^{(k)}, Z^{(k)})$ is sampled from joint distribution $p(S, Z)$ while $(S^{(k)}, Z^{(m)})$ is independently sampled from the marginal distributions $p(S)$ and $p(Z)$, respectively².

²In practice, we sample $(S^{(k)}, Z^{(m)})$ by randomly permuting $(S^{(k)}, Z^{(k)})$ pairs sampled from the joint distribution.

Minimizing $I(G; S)$. Note that the entropy of explanatory subgraph $H(S) = \mathbb{E}_{p(S)}[-\log p(S)]$ provides an upper bound for $I(G; S)$ since the inequality $I(G; S) = H(S) - H(S|G) \leq H(S)$ holds. However, it is intractable to calculate the entropy because the prior distribution of S is unknown in practice. To address this issue, we consider a relaxation and assume that the explanatory graph is a Gilbert random graph [34] where edges are conditionally independent to each other. Specifically, let $(i, j) \in \mathcal{E}$ denote the edge of graph G , and $e_{i,j} \sim \text{Bernoulli}(\mu_{i,j})$ be a binary variable indicating whether the edge (i, j) is selected for subgraph S . Thus, the probability of subgraph S is factorized as $p(S) = \prod_{(i,j) \in \mathcal{E}} p(e_{i,j})$, where $p(e_{i,j}) = \mu_{i,j}^{e_{i,j}} (1 - \mu_{i,j})^{1-e_{i,j}}$. In this way, we can arrive at an approximate upper bound for $I(G; S)$ with Monte Carlo sampling, which is denoted by

$$\mathcal{L}_2(S) = -\frac{1}{K} \sum_{k=1}^K \sum_{(i,j) \in \mathcal{E}} e_{i,j}^{(k)} \log \mu_{i,j}^{(k)} + (1 - e_{i,j}^{(k)}) \log(1 - \mu_{i,j}^{(k)}) \quad (7)$$

The reparameterization trick. Gradients-based optimization methods may fail to optimize Eq. (6) and Eq. (7) because of the non-differentiable sampling process and the discrete nature of subgraph structure. On this account, we follow the Gumbel-Softmax reparametrization trick [35, 36] and relax the binary variables $e_{i,j}$ to a continuous edge weight variables $\hat{e}_{i,j} = \sigma((\log \epsilon - \log(1 - \epsilon) + w_{i,j})/\tau) \in [0, 1]$, where $\sigma(\cdot)$ is the sigmoid function; $\epsilon \sim \text{Uniform}(0, 1)$; τ is the temperature hyper-parameter such that $\lim_{\tau \rightarrow 0} p(\hat{e}_{i,j} = 1) = \sigma(w_{i,j})$; $w_{i,j}$ is the latent variables which is calculated by a neural network following previous work [10],

$$w_{i,j}^{(k)} = \text{MLP}_{\theta_1} \left(\mathbf{z}_i^{(k)} \parallel \mathbf{z}_j^{(k)} \right) \text{ with } \mathbf{z}_i^{(k)} = \text{GNN}_{\theta_2} \left(G^{(k)}, i \right), i = 1, 2, \dots \quad (8)$$

where $\mathbf{z}_i^{(k)}$ denotes the node representations of node i . For better representation, we denote $\theta = \{\theta_1, \theta_2\}$, and generate the relaxed subgraph \hat{S} by $\hat{S}^{(k)} = g_{\theta}(G^{(k)})^3$. Let $\mu_{i,j}^{(k)} = \sigma(w_{i,j}^{(k)})$, the objective in Eq. (7) can be rewritten as

$$\mathcal{L}_2 \left(g_{\theta} \left(G^{(k)} \right) \right) = -\frac{1}{K} \sum_{k=1}^K \sum_{(i,j) \in \mathcal{E}} \hat{e}_{i,j}^{(k)} \log \sigma \left(w_{i,j}^{(k)} \right) + (1 - \hat{e}_{i,j}^{(k)}) \log \left(1 - \sigma \left(w_{i,j}^{(k)} \right) \right). \quad (9)$$

In summary, we rewrite the USIB optimization problem Eq. (3) as

$$\max_{\phi, \theta} \mathcal{L}_{USIB}(\phi, \theta, G) = \mathcal{L}_1 \left(\phi, g_{\theta} \left(G^{(k)} \right) \right) - \beta * \mathcal{L}_2 \left(g_{\theta} \left(G^{(k)} \right) \right). \quad (10)$$

An overview of our method is shown in Fig. 2. We first generate the explanatory subgraphs by a neural network, then another network is involved to estimate the mutual information between explanatory subgraphs and graph representations. Finally, the subgraph generator and the mutual information estimator are optimized collaboratively. The final explanatory subgraphs can be achieved by selecting edges with the top- n edge weights (*i.e.*, $\hat{e}_{i,j}^{(k)}$). Detailed algorithms can be found in the Appendix.

5 Theoretical analysis

In this section, we theoretically analyze the connection between representations and explanatory subgraphs on the label space. Before analyzing the connection, we first introduce two definitions to evaluate the expressiveness and robustness of representations.

Definition. Sufficiency: Considering a specific downstream task with label Y , the representation Z of graph G is sufficient for Y if and only if $I(G; Y|Z) = 0$.

A sufficient representation Z indicates that it is capable of predicting Y at least as accurately as the original graph G . Based on this definition, Proposition 1 holds (see proof in Appendix B).

Proposition 1. Let G and Y be random variables with joint distribution $p(G, Y)$, and Z be a representation of G . Considering a Markov Chain $Y \rightarrow G \rightarrow Z$, we assume that Z is conditionally independent from Y once G is given. Then, Z is sufficient for Y if and only if $I(Z; Y) = I(G; Y)$.

³ g_{θ} computes $w_{i,j}$ first and then generates the subgraph $\hat{S}^{(k)}$ by combining the relaxed edge weights and $G^{(k)}$ into a weighted graph.

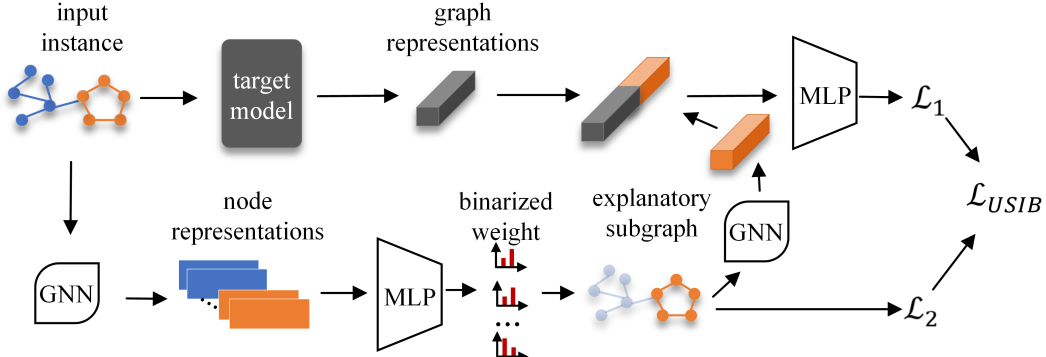


Figure 2: An illustration of our proposed USIB.

The *sufficiency* of representations evaluates the expressiveness of unsupervised representations, *i.e.*, for graph representations that are sufficient for a specific task, no information regarding the task is lost in the embedding procedure. Thus the unsupervised representations are expressive enough for the task.

Definition. Necessity: *Considering a specific downstream task with label Y , the representation Z of graph G is necessary for Y if and only if $I(G; Z|Y) = 0$.*

A necessary representation indicates that Z only extracts information relevant to Y from the graph G . According to this definition, the following Proposition 2 holds (see proof in Appendix B).

Proposition 2. *Let G and Y be random variables with joint distribution $p(G, Y)$, and Z be a representation of G . Considering a Markov Chain: $(G_N, Y) \rightarrow G \rightarrow Z$ where G_N collects all label-irrelevant information in G , Z is necessary for Y if and only if $I(G_N; Z) = 0$.*

The *necessity* of representations evaluates the robustness of unsupervised representations, *i.e.*, graph representations are unacted on label-irrelevant information, and thus the representations can be robust against noise information.

Given the definition of *sufficiency* and *necessity*, we have the following Theorem 1 that provides a theoretical connection between the graph representations and explanatory subgraphs on the label space (see proof in Appendix B).

Theorem 1. *Let G and Y be random variables with joint distribution $p(G, Y)$. Given unsupervised graph representation Z and its explanations S in graph G , we assume that S is conditionally independent from Y and Z when G is observed. We have,*

1. *if Z is sufficient for Y , then $I(S; Z) \geq I(S; Y)$;*
2. *if Z is necessary for Y , then $I(S; Z) \leq I(S; Y)$;*
3. *if Z is sufficient and necessary for Y , then $I(S; Z) = I(S; Y)$;*

Theorem 1 provides theoretical support for our USIB explanation method, *i.e.*, for representations that are expressive and robust enough, one can explore explanatory subgraphs that are highly relevant to the ground-truth labels by maximizing the mutual information between representations and explanatory subgraphs. In contrast, if representations are uninformative and fragile, the fidelity of explanatory subgraphs is not guaranteed. We experimentally analyze the influence of representations' expressiveness and robustness in the next section.

6 Experiments

In this section, we empirically evaluate the effectiveness and superiority of our proposed method by answering the following questions.

- **RQ1** How does our proposed method perform compared to other baseline explainers?
- **RQ2** Does expressiveness and robustness of representations affect the fidelity of explanatory subgraphs in agreement with the theoretical analysis?

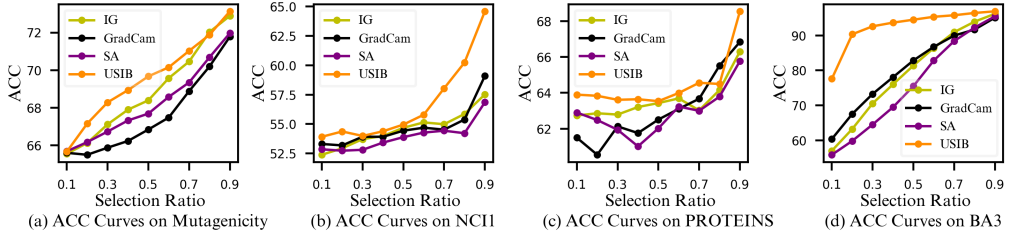


Figure 3: ACC curve of different explainers on Infograph.

6.1 Experimental settings

Datasets. We take four benchmark datasets for experiments, including Mutagenicity, NCI1, PROTEINS [37], and BA3 [25]. The first two are molecule graph datasets, while PROTEINS is a bioinformatics graph dataset. BA3 is a synthetic dataset created by Wang *et al.* [25]. Specifically, the Barabasi-Albert (BA) graphs are adopted as the base and attach each base with one of three motifs: house, cycle, and grid. The statistical details for these datasets can be found in Appendix D.

Target models. We consider three state-of-the-art target models to generate graph representations for explanation: Infograph [28], GCL [28], and ADGCL [29]. Note that all these target models adopt the same GNN encoder architecture for a fair comparison. The details of implementation can be found in Appendix D.

Baselines. To our best knowledge, there is no previous work focusing on the explanation for unsupervised graph representation learning. We train an MLP classifier based on representations generated by the target models and then compose the target models and the classifiers as end-to-end graph classifiers. Following this strategy, previous explanation methods for supervised setting, such as GNNExplainer [9], PGExplainer [10], PGM-Explainer [14], and Refine [25], could be adopted as baselines. Moreover, to provide a fair comparison without the involvement of label information, we also adapt several typical explanation methods for CNNs to our unsupervised graph representation explanation setting. Specifically, we adopt three methods which involve gradient-like scores by conducting backpropagation from the representations’ l_2 norm to the input, such as IG [23], GradCam [12], and SA [21].

Evaluation metrics. It is challenging to evaluate explanatory subgraphs quantitatively because the ground-truth explanations in practice are usually unreachable. Following previous works [9, 25, 38, 39], we adopt the following two metrics: (1) *Predictive Accuracy (ACC@r)*. For the explanatory subgraphs, which are crucial for the target GNN encoders, the corresponding subgraph representations should behave similarly to representations of the original graph on downstream tasks, *e.g.*, graph classification. To evaluate the fidelity of explanatory subgraphs, we feed the subgraphs to the target models first and get the subgraph representations. Then we train logistic classifiers on the subgraph representations and report the 10-fold cross-validation accuracy as ACC@ r for explanatory subgraphs with edge selection ratio r . Moreover we further denote ACC-AUC as the area under the ACC curve over different selection ratios $r \in \{0.1, 0.2, \dots, 0.9\}$. (2) *Recall@n*. Ground-truth explanations for the synthetic dataset BA3 are reachable. Thus we adopt the recall metric to evaluate explanatory subgraphs. It is formulated as Recall@ $n = \mathbb{E}_S [|S \cap S^*| / |S^*|]$, where n is the number of edges involved in the explanatory subgraphs; S^* denotes the ground-truth explanations. Note that each experiment is repeated 10 times to reduce randomness.

6.2 Quantitative evaluations

Effectiveness of USIB. To investigate the effectiveness of our proposed USIB explanation method, we present the ACC curve over different selection ratios in Fig. 3, and report the results on ACC-AUC and Recall@5 in Table 1. We only present the results on Infograph because of page limitation and present the results on other target models in Appendix D. The experimental results show that our proposed USIB achieves superior performance in the unsupervised setting and is comparable to baseline methods in the supervised setting. Specifically, USIB achieves the best performance on

Table 1: Comparison of our USIB and other baseline explainers. The relative improvement is calculated on unsupervised setting methods. **Bold** indicates the best results.

Target Model	Setting	Method	Mutagenicity		PROTEINS		BA3	
			ACC-AUC	ACC-AUC	ACC-AUC	ACC-AUC	ACC-AUC	Recall@5
Supervised	Infograph	PG-Explainer	69.29 \pm 2.10	59.93 \pm 1.42	65.50 \pm 2.32	89.99 \pm 3.81	26.49 \pm 3.27	
		GNNExplainer	68.99 \pm 2.08	54.68 \pm 1.34	62.16 \pm 2.20	74.78 \pm 3.94	18.80 \pm 0.92	
		PGM-Explainer	66.93 \pm 0.42	54.80 \pm 1.26	64.64 \pm 1.97	83.70 \pm 1.85	24.76 \pm 0.07	
		ReFine	67.45 \pm 0.97	57.88 \pm 1.30	66.28 \pm 1.66	84.78 \pm 6.59	17.88 \pm 8.79	
Unsupervised	Infograph	IG	68.87 \pm 1.52	54.65 \pm 0.94	63.30 \pm 2.25	79.52 \pm 2.18	16.22 \pm 5.11	
		GradCam	67.60 \pm 0.93	54.79 \pm 0.71	63.12 \pm 2.36	80.62 \pm 3.84	18.74 \pm 1.74	
		SA	68.24 \pm 0.97	53.94 \pm 0.65	62.71 \pm 2.16	76.02 \pm 3.07	16.35 \pm 3.01	
		USIB	69.55 \pm 0.96	56.70 \pm 1.65	64.46 \pm 2.75	92.55 \pm 3.28	27.16 \pm 4.46	
Relative Improvement			0.99%	3.49%	1.83%	14.80%	44.93%	

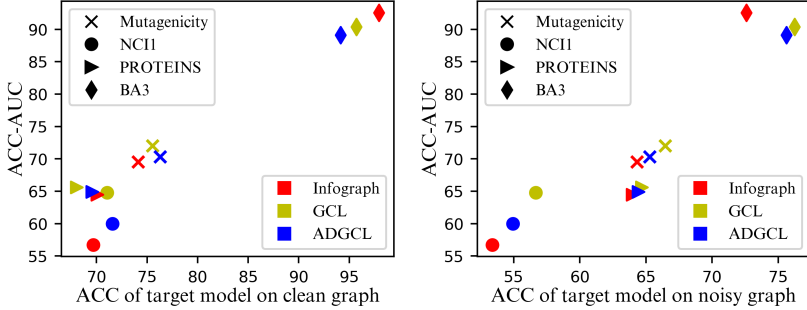


Figure 4: Influence of target models’ expressiveness and robustness. We distinguish different target models and datasets with different colors and markers separately.

Mutagenicity and BA3 among all baseline methods and outperforms other unsupervised methods on NCI1 and PROTEINS. However, there is still a gap between our USIB and supervised baseline methods on NCI1 and PROTEINS because of the involvement of label information. It is noteworthy that a significant relative improvement is achieved (*i.e.*, 14.8% on ACC-AUC and 10.44% on Recall@5) on the synthetic dataset BA3. It indicates that the performance of USIB is related to the expressiveness of target models (three target models achieve more than 90% ACC on BA3, which is much better than other datasets).

Influence of representations’ expressiveness and robustness. We quantitatively evaluate the expressiveness and robustness by the downstream graph classification accuracy (*i.e.*, ACC) on representations extracted respectively from the clean graphs and noisy graphs. The noisy graphs are generated by randomly adding $|\mathcal{E}|$ noise edges to the clean graphs. To investigate how representations’ expressiveness and robustness affect the fidelity of explanatory subgraphs, we show a scatter diagram in Fig. 4, where each point denotes a target model on a specific dataset. From Fig. 4, we can observe that: (1) There is a positive correlation between representations’ expressiveness/robustness and explanatory subgraphs’ fidelity. Representations achieving higher ACC on clean and noisy graphs usually lead to explanatory subgraphs with higher ACC-AUC. This observation is consistent with our theoretical analysis. (2) Expressiveness matters more than robustness when there is a significant gap on expressiveness. For example, we can observe that the fidelity of explanatory subgraphs on BA3 is positively related to the expressiveness while robustness makes less influence. (3) Robustness matters when there is only a slight gap on expressiveness. Specifically, the fidelity of explanatory subgraphs on Mutagenicity, NCI1, and PROTEINS is positively related to representations’ robustness since there is only a slight gap of expressiveness over clean graphs.

6.3 Qualitative analysis

We present the qualitative results on the synthetic dataset BA3 in Fig. 5. Specifically, we compare the explanation results of our USIB on untrained Infograph and fine-tuned Infograph qualitatively. We can clearly observe that the untrained Infograph focuses more on the random base graph. This can be attributed that the untrained Infograph recursively incorporates node’s information with

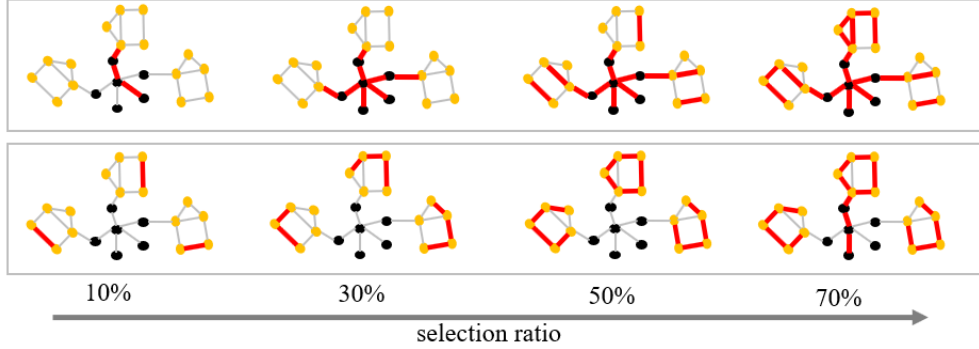


Figure 5: Qualitative results in BA3. The first row shows the explanation results of USIB on untrained Infograph, while the second row is the explanation results on fine-tuned Infograph. The yellow nodes denote the house motifs and the black nodes denote the random base graph. Explanation edges are colored as red.

random weights, and thus pays more attention to the central nodes in the graph, *i.e.*, the base graph. In contrast, the second row shows that the fine-tuned Infograph transfers its attention to the house motifs after the unsupervised training, which reveals why representations perform well on the downstream tasks. Moreover, we surprisingly find that Infograph’s performance does not rely on the completeness of motifs, *e.g.*, Infograph performs well even with only 30% edges according to Fig. 3. A rational explanation is the redundancy of graph information, *i.e.*, node features may preserve redundant information that is also contained in structural features. The redundancy may jeopardize the evaluation of explanation methods [40]. We consider it a future direction to construct datasets carefully designed for unsupervised graph representation explanation. We can also observe a limitation of USIB that it considers edges independently but ignores the substructures of graphs whose importance is emphasized in previous work [41].

7 Conclusion and future work

We study an unexplored explanation problem: the explanation for unsupervised graph representation learning. We advance the IB principle to tackle the explanation problem, which leads to a novel explanation method USIB. Moreover, we theoretically analyze the connection between representations and explanatory subgraphs on the label space, which reveals that expressiveness and robustness benefit the fidelity of explanatory subgraphs. Extensive results on four datasets and three target models demonstrate the superiority of our methods and the validity of our theoretical analysis. As a future direction, we consider the counterfactual explanation [42] for unsupervised representation learning and explore whether there is a connection between explanation and adversarial examples [43, 44, 45].

References

- [1] T. N. Kipf and M. Welling, “Semi-supervised classification with graph convolutional networks,” in *International Conference on Learning Representations (ICLR)*, 2017.
- [2] P. Veličković, G. Cucurull, A. Casanova, A. Romero, P. Liò, and Y. Bengio, “Graph Attention Networks,” *International Conference on Learning Representations*, 2018, accepted as poster. [Online]. Available: <https://openreview.net/forum?id=rJXMpikCZ>
- [3] M. Liu, H. Gao, and S. Ji, “Towards deeper graph neural networks,” in *Proceedings of the 26th ACM SIGKDD international conference on knowledge discovery & data mining*, 2020, pp. 338–348.
- [4] W. Hamilton, Z. Ying, and J. Leskovec, “Inductive representation learning on large graphs,” *Advances in neural information processing systems*, vol. 30, 2017.
- [5] Z. Ying, J. You, C. Morris, X. Ren, W. Hamilton, and J. Leskovec, “Hierarchical graph representation learning with differentiable pooling,” *Advances in neural information processing systems*, vol. 31, 2018.

- [6] K. Xu, W. Hu, J. Leskovec, and S. Jegelka, “How powerful are graph neural networks?” in *International Conference on Learning Representations*, 2019. [Online]. Available: <https://openreview.net/forum?id=ryGs6iA5Km>
- [7] M. Zhang and Y. Chen, “Link prediction based on graph neural networks,” *Advances in neural information processing systems*, vol. 31, 2018.
- [8] L. Cai, J. Li, J. Wang, and S. Ji, “Line graph neural networks for link prediction,” *IEEE Transactions on Pattern Analysis and Machine Intelligence*, 2021.
- [9] Z. Ying, D. Bourgeois, J. You, M. Zitnik, and J. Leskovec, “Gnnexplainer: Generating explanations for graph neural networks,” *Advances in neural information processing systems*, vol. 32, 2019.
- [10] D. Luo, W. Cheng, D. Xu, W. Yu, B. Zong, H. Chen, and X. Zhang, “Parameterized explainer for graph neural network,” *Advances in neural information processing systems*, vol. 33, pp. 19 620–19 631, 2020.
- [11] F. Doshi-Velez and B. Kim, “Towards a rigorous science of interpretable machine learning,” *arXiv preprint arXiv:1702.08608*, 2017.
- [12] P. E. Pope, S. Kolouri, M. Rostami, C. E. Martin, and H. Hoffmann, “Explainability methods for graph convolutional neural networks,” in *Proceedings of the IEEE/CVF Conference on Computer Vision and Pattern Recognition*, 2019, pp. 10 772–10 781.
- [13] H. Yuan, H. Yu, S. Gui, and S. Ji, “Explainability in graph neural networks: A taxonomic survey,” *arXiv preprint arXiv:2012.15445*, 2020.
- [14] M. Vu and M. T. Thai, “Pgm-explainer: Probabilistic graphical model explanations for graph neural networks,” *Advances in neural information processing systems*, vol. 33, pp. 12 225–12 235, 2020.
- [15] B. Perozzi, R. Al-Rfou, and S. Skiena, “Deepwalk: Online learning of social representations,” in *Proceedings of the 20th ACM SIGKDD international conference on Knowledge discovery and data mining*, 2014, pp. 701–710.
- [16] J. Tang, M. Qu, M. Wang, M. Zhang, J. Yan, and Q. Mei, “Line: Large-scale information network embedding,” in *Proceedings of the 24th international conference on world wide web*, 2015, pp. 1067–1077.
- [17] A. Grover and J. Leskovec, “node2vec: Scalable feature learning for networks,” in *Proceedings of the 22nd ACM SIGKDD international conference on Knowledge discovery and data mining*, 2016, pp. 855–864.
- [18] T. N. Kipf and M. Welling, “Variational graph auto-encoders,” *NIPS Workshop on Bayesian Deep Learning*, 2016.
- [19] J. Yu, T. Xu, Y. Rong, Y. Bian, J. Huang, and R. He, “Recognizing predictive substructures with subgraph information bottleneck,” *IEEE Transactions on Pattern Analysis and Machine Intelligence*, 2021.
- [20] T. Wu, H. Ren, P. Li, and J. Leskovec, “Graph information bottleneck,” *Advances in Neural Information Processing Systems*, vol. 33, pp. 20 437–20 448, 2020.
- [21] F. Baldassarre and H. Azizpour, “Explainability techniques for graph convolutional networks,” in *International Conference on Machine Learning (ICML) Workshops, 2019 Workshop on Learning and Reasoning with Graph-Structured Representations*, 2019.
- [22] T. Schnake, O. Eberle, J. Lederer, S. Nakajima, K. T. Schutt, K.-R. Mueller, and G. Montavon, “Higher-order explanations of graph neural networks via relevant walks,” *IEEE Transactions on Pattern Analysis and Machine Intelligence*, 2021.
- [23] M. Sundararajan, A. Taly, and Q. Yan, “Axiomatic attribution for deep networks,” in *International conference on machine learning*. PMLR, 2017, pp. 3319–3328.
- [24] P. Schwab and W. Karlen, “Cxplain: Causal explanations for model interpretation under uncertainty,” *Advances in Neural Information Processing Systems*, vol. 32, 2019.
- [25] X. Wang, Y.-X. Wu, A. Zhang, X. He, and T.-S. Chua, “Towards multi-grained explainability for graph neural networks,” in *Proceedings of the 35th Conference on Neural Information Processing Systems*, 2021.

[26] H. Yuan, J. Tang, X. Hu, and S. Ji, “Xgnn: Towards model-level explanations of graph neural networks,” in *Proceedings of the 26th ACM SIGKDD International Conference on Knowledge Discovery & Data Mining*, 2020, pp. 430–438.

[27] F.-Y. Sun, J. Hoffman, V. Verma, and J. Tang, “Infograph: Unsupervised and semi-supervised graph-level representation learning via mutual information maximization,” in *International Conference on Learning Representations*, 2019.

[28] Y. You, T. Chen, Y. Sui, T. Chen, Z. Wang, and Y. Shen, “Graph contrastive learning with augmentations,” in *Advances in Neural Information Processing Systems*, H. Larochelle, M. Ranzato, R. Hadsell, M. F. Balcan, and H. Lin, Eds., vol. 33. Curran Associates, Inc., 2020, pp. 5812–5823. [Online]. Available: <https://proceedings.neurips.cc/paper/2020/file/3fe230348e9a12c13120749e3f9fa4cd-Paper.pdf>

[29] S. Suresh, P. Li, C. Hao, and J. Neville, “Adversarial graph augmentation to improve graph contrastive learning,” *NeurIPS*, 2021.

[30] N. TISHBY, “The information bottleneck method,” in *Proc. 37th Annual Allerton Conference on Communications, Control and Computing, 1999*, 1999, pp. 368–377.

[31] N. Tishby and N. Zaslavsky, “Deep learning and the information bottleneck principle,” in *2015 ieee information theory workshop (itw)*. IEEE, 2015, pp. 1–5.

[32] R. D. Hjelm, A. Fedorov, S. Lavoie-Marchildon, K. Grewal, P. Bachman, A. Trischler, and Y. Bengio, “Learning deep representations by mutual information estimation and maximization,” in *International Conference on Learning Representations*, 2018.

[33] S. Nowozin, B. Cseke, and R. Tomioka, “f-gan: Training generative neural samplers using variational divergence minimization,” *Advances in neural information processing systems*, vol. 29, 2016.

[34] E. N. Gilbert, “Random graphs,” *The Annals of Mathematical Statistics*, vol. 30, no. 4, pp. 1141–1144, 1959.

[35] C. Maddison, A. Mnih, and Y. Teh, “The concrete distribution: A continuous relaxation of discrete random variables,” in *Proceedings of the international conference on learning Representations*. International Conference on Learning Representations, 2017.

[36] E. Jang, S. Gu, and B. Poole, “Categorical reparameterization with gumbel-softmax,” in *5th International Conference on Learning Representations, ICLR 2017, Toulon, France, April 24-26, 2017, Conference Track Proceedings*. OpenReview.net, 2017. [Online]. Available: <https://openreview.net/forum?id=rkE3y85ee>

[37] C. Morris, N. M. Kriege, F. Bause, K. Kersting, P. Mutzel, and M. Neumann, “Tudataset: A collection of benchmark datasets for learning with graphs,” in *ICML 2020 Workshop on Graph Representation Learning and Beyond (GRL+ 2020)*, 2020. [Online]. Available: www.graphlearning.io

[38] J. Chen, L. Song, M. Wainwright, and M. Jordan, “Learning to explain: An information-theoretic perspective on model interpretation,” in *International Conference on Machine Learning*. PMLR, 2018, pp. 883–892.

[39] J. Liang, B. Bai, Y. Cao, K. Bai, and F. Wang, “Adversarial infidelity learning for model interpretation,” in *Proceedings of the 26th ACM SIGKDD International Conference on Knowledge Discovery & Data Mining*, 2020, pp. 286–296.

[40] L. Faber, A. K. Moghaddam, and R. Wattenhofer, “When comparing to ground truth is wrong: On evaluating gnn explanation methods,” in *Proceedings of the 27th ACM SIGKDD Conference on Knowledge Discovery & Data Mining*, 2021, pp. 332–341.

[41] H. Yuan, H. Yu, J. Wang, K. Li, and S. Ji, “On explainability of graph neural networks via subgraph explorations,” in *International Conference on Machine Learning*. PMLR, 2021, pp. 12 241–12 252.

[42] A. Lucic, M. ter Hoeve, G. Tolomei, M. de Rijke, and F. Silvestri, “Cf-gnnexplainer: Counterfactual explanations for graph neural networks,” *arXiv preprint arXiv:2102.03322*, 2021.

[43] D. Zügner, A. Akbarnejad, and S. Günnemann, “Adversarial attacks on neural networks for graph data,” in *Proceedings of the 24th ACM SIGKDD International Conference on Knowledge Discovery & Data Mining*, 2018, pp. 2847–2856.

- [44] H. Dai, H. Li, T. Tian, X. Huang, L. Wang, J. Zhu, and L. Song, “Adversarial attack on graph structured data,” in *International conference on machine learning*. PMLR, 2018, pp. 1115–1124.
- [45] J. Wang, M. Luo, F. Suya, J. Li, Z. Yang, and Q. Zheng, “Scalable attack on graph data by injecting vicious nodes,” *Data Mining and Knowledge Discovery*, vol. 34, no. 5, pp. 1363–1389, 2020.

Robust Task-Oriented Dialogue Generation with Contrastive Pre-training and Adversarial Filtering

Shiquan Yang, Xinting Huang, Jey Han Lau, Sarah Erfani

The University of Melbourne, Australia

{shiquan@student., xintingh@student., laujh@, sarah.erfani@unimelb.edu.au}

ABSTRACT

Data artifacts incentivize machine learning models to learn non-transferable generalizations by taking advantage of shortcuts in the data, and there is growing evidence that data artifacts play a role for the strong results that deep learning models achieve in recent natural language processing benchmarks. In this paper, we focus on task-oriented dialogue and investigate whether popular datasets such as MultiWOZ contain such data artifacts. We found that by only keeping frequent phrases in the training examples, state-of-the-art models perform similarly compared to the variant trained with full data, suggesting they exploit these spurious correlations to solve the task. Motivated by this, we propose a contrastive learning based framework to encourage the model to ignore these cues and focus on learning generalisable patterns. We also experiment with adversarial filtering to remove “easy” training instances so that the model would focus on learning from the “harder” instances. We conduct a number of generalization experiments — e.g., cross-domain/dataset and adversarial tests — to assess the robustness of our approach and found that it works exceptionally well.

ACM Reference Format:

Shiquan Yang, Xinting Huang, Jey Han Lau, Sarah Erfani, The University of Melbourne, Australia, {shiquan@student., xintingh@student., laujh@, sarah.erfani@unimelb.edu.au} . 2022. Robust Task-Oriented Dialogue Generation with Contrastive Pre-training and Adversarial Filtering. In *Proceedings of (XXXXXX)*. ACM, New York, NY, USA, 11 pages. <https://doi.org/XXXXXX.XXXXXXX>

1 INTRODUCTION

Task-oriented dialogue systems aim to help human accomplish certain tasks such as restaurant reservation or navigation via natural language utterances. Recently, pre-trained language models [19, 32, 45] achieve impressive results on dialogue response generation and knowledge base (KB) reasoning, two core components of dialogue systems. However, neural networks are found to be prone to learning *data artifacts* [21, 28], i.e. superficial statistical patterns in the training data, and as such these results may not generalise to more challenging test cases, e.g., test data that is drawn from a different distribution to the training data.

Permission to make digital or hard copies of all or part of this work for personal or classroom use is granted without fee provided that copies are not made or distributed for profit or commercial advantage and that copies bear this notice and the full citation on the first page. Copyrights for components of this work owned by others than ACM must be honored. Abstracting with credit is permitted. To copy otherwise, or republish, to post on servers or to redistribute to lists, requires prior specific permission and/or a fee. Request permissions from permissions@acm.org.

XXXXXX, XXXXXX, XXXXXX

© 2022 Association for Computing Machinery.

ACM ISBN 978-x-xxxx-xxxx-x/YY/MM...\$15.00

<https://doi.org/XXXXXX.XXXXXXX>

This issue has been documented in several natural language processing (NLP) tasks [3, 28, 30]. For example, in natural language inference (NLI), where the task is to determine whether one given sentence entails the other, the models trained on NLI benchmark datasets are highly likely to assign a “contradiction” label if there exists a word *not* in the input sentences even if the true relation is “entailment”, as *not* often co-occurs with the label “contradiction” in the training set. Similar issues have also been observed in many other tasks such as commonsense reasoning [3], visual question answering [29, 35], and argument reasoning [30]. However, it’s unclear whether such shortcuts exist in popular task-oriented dialogue datasets such as MultiWOZ [10], and whether existing dialogue models are genuinely learning the underlying task or exploiting biases¹ hidden in the data.

To investigate this, we start by probing whether state-of-the-art dialogue models are discovering and exploiting spurious correlations on a popular task-oriented dialogue dataset. Specifically, we measure two state-of-the-art dialogue models’ performance under two different configurations: full input (original dialogue history, e.g., *I need to find a moderately priced hotel*) and partial input (dialogue history that contains only frequent phrases, e.g., *I need to*). Preliminary experiments found that these models perform similarly under the two configurations, suggesting that these models have picked up these cues — frequent word patterns which are often not meaning bearing — to make predictions. This implies that these models did not learn transferable generalizations for the task, and will likely perform poorly on *out-of-distribution* test data, e.g., one that has a different distribution to the training data.

To address this, we decompose task-oriented dialogue into two task: delexicalized response generation and KB reasoning (prediction of the right entities in the response), and explore methods to improve model robustness for the latter. Using frequent phrases as the basis of dataset bias, we experiment with contrastive learning to encourage the model to ignore these phrases to focus on meaning bearing words. Specifically, we pre-train our language model with a contrastive objective to encourage it to learn a similar representation for an original input (e.g., *I need to find a moderately priced hotel*) and its debiased pair (e.g., *find a moderately priced hotel*) before fine-tuning it for KB entity prediction.

Another source of bias comes from the data distribution [3]. We found that the KB entity distribution in MultiWOZ can be highly skewed in certain contexts, e.g., if the dialogue context starts with *I need to*, the probability of the KB entity *Cambridge* substantially exceeds chance level, which leads to inadequate learning of entities in the tail of the distribution. Here we adapt an adversarial filtering algorithm [39] to our task, which filters “easy samples” (i.e., samples

¹We use the terms *artifacts*, *biases*, *cues* and *shortcuts* to denote the same concept and use them interchangeably throughout the paper.

in the head of the distribution) in the training data to create a more balanced data distribution so as to encourage the model to learn from the tail of the distribution.

We conduct a systematic evaluation on the robustness of our method and four state-of-the-art task-oriented dialogue systems under various out-of-distribution settings. Experimental results demonstrate that our method substantially outperforms these benchmark systems.

To summarize, our contributions are as follows:

- We conduct analysis on a popular task-oriented dialogue dataset and reveal shortcuts based on frequent word heuristics.
- We propose a two-stage contrastive learning framework to debias spurious cues in the model inputs, and adapt adversarial filtering to create a more balanced training data distribution to improve the robustness of our task-oriented dialogue system.
- We perform comprehensive experiments to validate the robustness of our method against a number of strong benchmark systems in various out-of-distribution test settings and found our method substantially outperforms its competitors.

2 RELATED WORK

2.1 Task-oriented Dialogue

Traditionally, task-oriented dialogue systems are built via pipeline based approach where four independently designed and trained modules are connected together to generate the final system responses. These include natural language understanding [7], dialogue state tracking [46, 53], policy learning [34], and natural language generation [6]. However, the pipeline based approach can be very costly and time-consuming as each module needs module-specific training data and can not be optimized in a unified way. To address this, many end-to-end approaches [2, 24, 27] have been proposed to reduce human efforts in recent years. Lei et al. [24] propose a two-stage sequence-to-sequence model to incorporate dialogue state tracking and response generation jointly in a single sequence-to-sequence architecture. Wu et al. [47] propose a global-local pointer mechanism that trains a global pointer at encoding stage using multi-task learning with addition supervisions extracted from the system responses. Qin et al. [36] use a shared-private sequence-to-sequence architecture to handle the transferability of the system on KB incorporation and response generation. Zhang et al. [51] propose a domain-aware multi-decoder network to combine belief state tracking, action prediction and response generation in a single neural architecture. More recently, the field has shifted towards using large-scale pre-trained language models such as BERT [9] and GPT-2 [37] for task-oriented dialogue modeling due to their success on many NLP tasks [32, 44, 52]. Peng et al. [32] and Hosseini-Asl et al. [19] employed a GPT-2 based model jointly trained for belief state prediction and response generation in a multi-task fashion. Wu et al. [45] pre-train BERT on multiple task-oriented dialogue datasets for response selection.

2.2 Spurious Cues in NLP data

Deep neural networks have achieved tremendous progress on many NLP tasks [15, 20, 43, 48, 49] with the emergence of large-scale pre-trained language models like BERT [8] and GPT-2 [37]. However, many recent NLP studies [3, 18, 21, 28, 30] have found that deep neural networks are prone to exploit spurious artifacts present in the data rather than learning the underlying task. In natural language inference (NLI), [1] found that certain linguistic phenomenon in the NLI benchmark datasets correlate well with certain classes. For example, by only looking at the hypothesis, simple classifier models can perform as well as the model using full inputs (both hypothesis and premise). [30] found that BERT achieves a performance close to human on Argument Reasoning Comprehension Task (ARCT) with 77% accuracy (3% below human performance). However, they discover that the impressive performance is attributed to the exploitation of shortcuts in the dataset. [14] analyze annotator bias on NLP datasets and found that a model that uses only annotator identifiers can achieve a similar performance to one that uses the full data. In commonsense reasoning, [3] has performed a systematic investigation over four commonsense related tasks and found that most datasets experimented with are problematic with models are prone to leveraging the non-robust features in the inputs to make decisions and do not generalize well to the overall tasks intended to be conveyed by the commonsense reasoning tasks and datasets. Inspired by these studies, our paper focus on analyzing data artifacts in task-oriented dialogue datasets.

2.3 Bias Reduction in NLP

To address the data artifact issue, several approaches have been proposed. In NLI, He et al. [17] propose to train a debiased classifier by fitting the residuals of a biased classifier trained using insufficient features. However, their approach relies on task-specific prior knowledge about the bias types such as hypothesis-only bias in NLI. Sanh et al. [40] propose to leverage a weak learner to automatically identify the biased examples in the training data and only use the hard examples to train the main model to obtain a debiased classifier. In commonsense reasoning, Sakaguchi et al. [39] propose AF-Lite that iteratively removes “easy” samples in the training data during model training to make model focus on the “hard” examples to improve the robustness of commonsense reasoning models. Note though, that their approach is designed for classification tasks, and as such is not straightforward to adapt them to task-oriented dialogue. We tackle this by decomposing the problem into the two sub-tasks: lexicalized dialogue generation and KB entity prediction, so that we can apply AF-lite to the latter (as it is a classification problem).

3 SPURIOUS CUES IN TASK-ORIENTED DIALOGUE DATASET

To unveil potential linguistic artifacts in task-oriented dialogue datasets, we first conduct an investigation on MultiWOZ [4], which is widely used among task-oriented dialogue studies. By comparing the performance of a model trained using full dialogue history (e.g., *I need to find a moderately priced hotel*) and partial history containing only frequent phrases (e.g., *I need to*), it tells us if shortcuts exist in the dataset and the model has picked them up to solve the task. Note

Model	Input Signals	F1	BLEU
SimpleTOD [19]	Full Input	35.80	20.20
SimpleTOD [19]	Frequent phrases only	34.33	19.63
GLMP [47]	Full Input	33.79	6.22
GLMP [47]	Frequent phrases only	32.68	6.18

Table 1: Performance of two dialogue models under two training settings: using full input or partial input containing only frequent phrases. F1 and BLEU measure the accuracy of entity prediction and quality of generated response respectively.

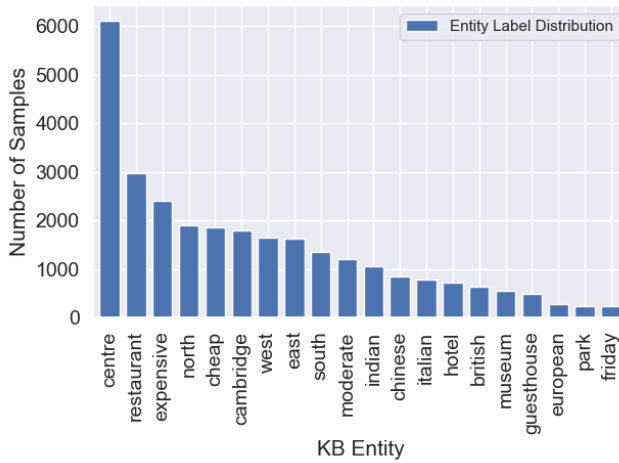


Figure 1: Entity label distribution on benchmark dataset MultiWOZ. X-axis denotes the top-20 most frequent entities in the system responses. Y-axis denotes the number of samples containing each entity.

that these frequent phrases tend to be function words that don't bear much meaning (e.g., *I need to*), and as such a model that can perform the task well using only them means it has not truly solved the task by capturing the underlying semantics of user utterances.

We experiment with two popular types of dialogue models based on GPT (SimpleTOD [19]) and recurrent networks (GLMP [47]). We evaluate using Entity F1 [11] and BLEU [31] metrics which are the two main metrics for assessing the performance of dialogue models. F1 measures the accuracy of the system's ability to extract the correct entities from the knowledge base, while BLEU measures how much word overlap between the system-generated response and the ground truth response; higher score means better performance in both metrics. The results are shown in Table 1. As we can see, both models perform similarly under the two training settings, implying that there are shortcuts in the data (i.e., frequent phrases that correlate strongly with entities and responses), and the model has learned to exploit these cues for the task. Manual analysis reveals that 87% of the frequent phrases do not contain much semantic information: most of them are made up of function words such as *I'm looking for*, *I would like*, *I don't care*, and *That is*

all. These results suggest that these models did not solve the task by having any real natural language understanding.

Next we look into class imbalance, another source of dataset biases [3]. We analyze the distribution of KB entities in the system responses, i.e., we tally how often each entity appears in the responses in MultiWOZ and plot a histogram of their frequencies in Figure 1. We find that the entity distribution is highly skewed, with the top-10 "head entities" (i.e., the most frequent entities) accounting for approximately 64% of total occurrences, which means a large portion of the entities are in the (very) long tail of the distribution. The implication is that a model can simply focus on learning from a small number of head entities to achieve a high performance. Motivated by this observation, we adapt filtering algorithms to tackle this class imbalance issue, which works by smoothing the distribution so as to encourage our model to learn not only from the head of the distribution but also from the tail.

4 MODEL ARCHITECTURE

4.1 Problem Formulation

We focus on the problem of task-oriented dialogue response generation with external knowledge base (KB). Formally, given the dialogue history D and knowledge base B , our goal is to generate the system responses Y in a word-by-word fashion. The probability of the generated responses can be written as:

$$p(Y|D, B) = \prod_{t=1}^n p(y_t|D, B, y_1, y_2, \dots, y_{t-1})$$

where y_t is the t -th token in the response Y .

4.2 Overview

We decompose the dialogue generation task into two sub-tasks: delexicalized response generation and entity prediction. The delexicalized response is the response where KB entities are substituted by placeholders to reduce the complexity of the problem through a smaller vocabulary. For example, in Figure 2, *Davinci Pizzeria* is replaced by "[restaurant_name]" in the response. We follow the delexicalization process proposed in [19]. We employ the two-phase design because it disentangles the entity prediction task from response generation task, allowing us to focus on bias reduction for entity prediction. Our framework uses a pre-trained autoregressive model (GPT-2) as the response generator and a pre-trained bidirectional encoder (BERT) as the entity predictor. Note that GPT-2 is fine-tuned to generate the delexicalized responses while the BERT model is fine-tuned to predict entities at every timestep during decoding, and the final response is created by replacing the placeholder tokens (generated by GPT-2) using the predicted entities (by BERT). Figure 2 presents the overall architecture. We first describe how the delexicalized response generation operates in Section 4.3 followed by entity prediction in Section 4.4. We introduce our debiasing techniques for the entity prediction model in Section 5.

4.3 Delexicalized Response Generation

We follow [19] and fine-tune GPT-2 to generate the delexicalized responses. Note that the input is always prefixed with the dialogue

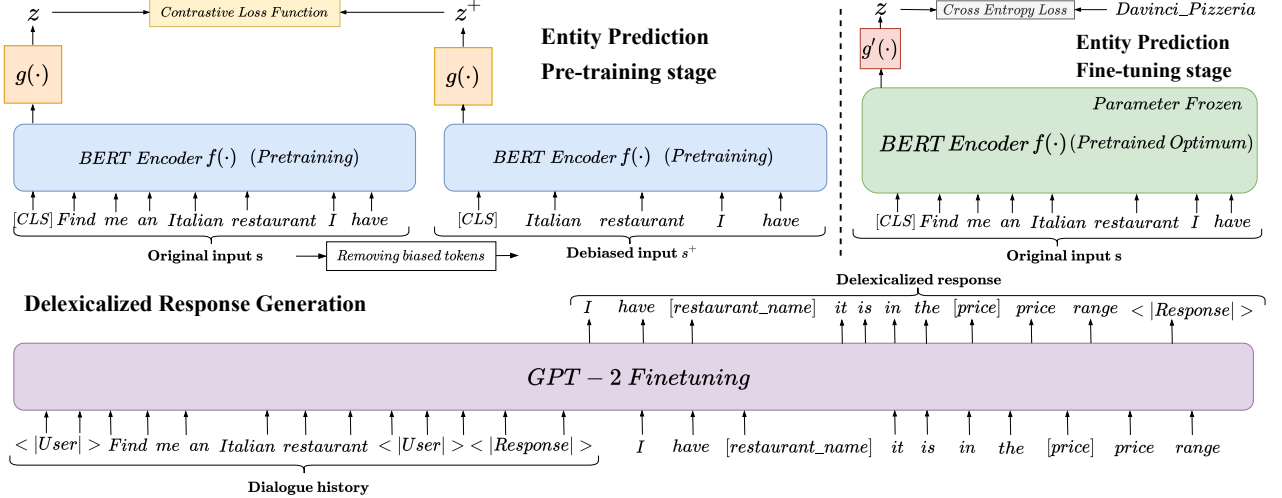


Figure 2: Overview of our proposed approach. The top shows the two-stage design for entity prediction: BERT pre-training using contrastive loss and fine-tuning using cross-entropy loss. The bottom shows the delexicalized response generation by fine-tuning GPT-2.

history and GPT-2 is fine-tuned via cross-entropy loss to predict the next (single turn) response.²

4.4 Entity Prediction

The entity prediction task can be formulated as a multi-class classification problem. The goal of the entity prediction module is to predict the correct KB entities at each timestep during the response generation process, given the dialogue context and the generated word tokens before current timestep. Formally, let $D = [x_1, x_2, \dots, x_n]$ be the dialogue history, $Y = [y_1, y_2, \dots, y_m]$ be the ground truth delexicalized response, where n is the number of tokens in the dialogue history, m the number of tokens in the response. During training, we fine-tune BERT to predict the entity at the t -th timestep, by taking the dialogue history and the generated tokens, i.e., $\bar{D} = [x_1, x_2, \dots, x_n, y_1, y_2, \dots, y_{t-1}]$, as the input:

$$\begin{aligned} H &= BERT_{enc}(\phi^{emb}(\bar{D})) \\ z &= g(H_{CLS}) \\ P &= \text{softmax}(z) \end{aligned}$$

where ϕ^{emb} is the embedding layer of BERT, H_{CLS} the hidden state of the [CLS] token, g a linear layer, and P the probability distribution over the KB entity set. Note that the KB entity set consists of all KB entities and a special label [NULL], which is used when the token to be predicted at timestep t is not an entity (i.e., normal words). During inference, we use the delexicalized response generated by GPT-2 as input, and at each time step select the entity with the largest probability produced by BERT as the output.

The delexicalized response generator (GPT-2) and entity predictor (BERT) are trained separately, and at test time we first generate

²To inform the model about user utterances and system utterances in the dialogue context, we add special tokens $<|user|>$ and $<|system|>$ at the beginning and end of user and system utterances for each turn of the dialogue history, following [19]. We also add a symbol $<|response|>$ at the end of the dialogue history to indicate the start of the response generation.

the delexicalized response and then use it as input to the entity predictor to predict the entities at every time step. Once that's done, we lexicalize the response by substituting the placeholder tokens with their corresponding entities to create the final response.

5 DEBIASED TRAINING FOR ROBUST ENTITY PREDICTION

Motivated by our preliminary findings a model that uses full input (*I need to find a moderately priced hotel*) performs similarly compared to one that uses filtered input containing only frequent phrases (*I need to*), we propose to use contrastive learning to encourage the entity predictor (BERT) to focus on the important semantic words, e.g., *find a moderately priced hotel* instead of *I need to*, during representation learning. We propose three methods leveraging n -gram statistics ($n = 3$): frequency (Section 5.1.1), mutual information (Section 5.1.2), and Jensen-Shannon divergence (Section 5.1.3).

Our approach integrates contrastive learning in the domain-adaptive pre-training stage [16]. That is, we take the off-the-shelf pre-trained BERT, and perform another step of pre-training to adapt it to our domain. Conventionally this domain-adaptive pre-training is done using masked language model loss, but we propose to use contrastive loss instead to encourage BERT to learn similar representations/encodings between the full input (*I need to find a moderately priced hotel*) and a debiased input (*find a moderately priced hotel*), thereby forcing the model to focus on the semantic words. After this contrastive pre-training, we fine-tune BERT for the entity prediction task as we described in Section 4.4.

Lastly, we also explore adapting an adversarial filtering algorithm [39] to further debias our model; this is detailed in Section 5.2.

5.1 Contrastive Learning

The core idea of contrastive learning is to learn representations where positive pairs are embedded in a similar space while negative

pairs are pushed apart as much as possible [13, 22, 42]. We follow the contrastive learning framework in [13] that takes a set of paired utterances $S = \{(s_i, s_i^+)\}_{i=1}^N$ as inputs, where s_i denotes the original input and s_i^+ denotes its positive counterparts (i.e., the debiased utterances). It employs in-batch negatives and cross-entropy loss for training. Formally, the inputs s_i and s_i^+ are first mapped into feature representations in vector space as z_i and z_i^+ . In our case we use BERT as our encoder to produce the features. The training loss \mathcal{L} for S , a minibatch with N pairs of utterances is:

$$\mathcal{L} = -\mathbb{E}_S \left[\log \frac{e^{\text{sim}(z_i, z_i^+)/\tau}}{\sum_{j=1}^N e^{\text{sim}(z_i, z_j^+)/\tau}} \right]$$

where τ is a temperature hyperparameter, sim the cosine similarity function. The critical issue of contrastive learning is to construct a *meaningful* positive counterpart, which in our case means capturing the semantic bearing words in the original utterance. We next describe three ideas to construct the positive pairs based on n -gram statistics.

5.1.1 Criterion-1: Frequent n -grams. We select the top-10% n -grams according to their frequency in the training data,³ and create positive pairs containing: (1) an original input (dialogue history and response up to timestep $t-1$); and (2) filtered input where frequent n -grams are removed. As explained earlier in Section 5, this simple approach forces BERT to learn a similar representation between the full input (*I need to find a moderately priced hotel*) and debiased input (*find a moderately priced hotel*) by removing these n -grams directly.

5.1.2 Criterion-2: Mutual Information. The previous approach does not consider the label information (i.e., the entities contained in the responses). To incorporate label information, we explore computing mutual information between n -grams and the entities. The idea is that we want to discover n -grams that produce strong correlation with entities, which means that BERT is likely to pick them up as shortcuts for prediction. Formally:

$$I(A; B) = \sum_{A,B} p(A, B) \log \frac{p(A|B)}{p(A)}$$

where A is an n -gram and B a target entity.

We rank all pairs of n -grams and entities this way, and select the top-10% pairs and use their n -grams (ignoring the entities) as the candidate set where we remove them in the input to create the positive pairs as before. The detailed algorithm is shown in Algorithm 1.

5.1.3 Criterion-3: Jensen-Shannon Divergence. The previous approach accounts for label (entity) information, but has the limitation where it considers only the *presence* of an n -gram with a target entity. Here we extend the approach to also consider the *absence* of the n -gram, and what impacts this brings to the appearance of the target entity. To this end we compute the Jensen-Shannon divergence of two probability distributions: (1) entity distribution where an n -gram is present in the input (P); and (2) entity distribution where an n -gram is absent in the input (Q). The idea is that an

³Recall that we perform entity prediction for every timestep in the response, and so for each response we have m training instances, where m is the number of tokens in the response.

n -gram is highly informative (in terms of predicting the entities) if the divergence of the distributions is high, and we want to remove these n -grams from the input. Formally:

$$JSD(P; Q) = \frac{1}{2} \sum_{x \in \mathbb{X}} P(x) \log \frac{P(x)}{M(x)} + \frac{1}{2} \sum_{x \in \mathbb{X}} Q(x) \log \frac{Q(x)}{M(x)}$$

where P and Q are two probability distributions over \mathbb{X} , $M = 1/2 (P+Q)$. Details about the algorithm are shown in Algorithm 2. As before, we select the top-10% n -grams ranked by the divergence values as the candidate n -grams to filter in the input.

Algorithm 1: Mutual information based bias identification

```

Input : dataset  $\mathcal{D} = (\mathbf{X}, \mathbf{y})$ ,  $n$ -gram size  $n$ , cutoff size  $k$ 
Output: biased tokens set  $\mathcal{S}$ 
1 Initialize  $n$ -grams distribution  $P_{ngrams} \leftarrow \emptyset$ ;
2 Initialize entity distribution  $P_{entity} \leftarrow \emptyset$ ;
3 Initialize ngrams-entity joint distribution  $P_{joint} \leftarrow \emptyset$ ;
4 Initialize mutual information values  $Q \leftarrow \emptyset$ ;
5 foreach  $(x, y) \in (\mathbf{X}, \mathbf{y})$  do
6    $ngrams \leftarrow \text{FindNgrams}(x, n)$ ;
7   foreach element  $e$  of the  $ngrams$  do Add  $e$  to  $P_{ngrams}$ ;
8   Add  $y$  to  $P_{entity}$ ;
9   forall  $e \in ngrams$  do Add  $(e, y)$  to  $P_{joint}$ ;
10 end
11 forall  $(e_1, e_2) \in P_{joint}$  do
12   Calculate mutual information  $m$  of  $(e_1, e_2)$  using
       $P_{ngrams}, P_{entity}, P_{joint}$  with Equation 5.1.2;
13   Add  $(e_1, e_2, m)$  to  $Q$ ;
14 end
15 Select the top- $k$  elements  $\mathcal{F}$  of  $Q$  and Add  $\mathcal{F}(e_1)$  to  $\mathcal{S}$ ;
16 return  $\mathcal{S}$ 

```

5.2 Adversarial Filtering

Contrastive pre-training identifies and eliminates biased tokens at the input representation level. However, this does not change the entity label distribution, which is another source of bias that makes deep learning models brittle to unseen scenarios [25, 33]. To address this, we adapt the adversarial filtering proposed by [39] to smooth the entity label distribution to prevent the model from learning only from the head of the distribution (frequent entities) but also from the tail of the distribution (rarer entities). The core idea of adversarial filtering is to filter out “easy” training examples – training instances where their removal doesn’t negatively impact the model – to encourage the model to learn from the “hard” examples, through an iterative process utilizing weak linear learners.

During each iteration, we train 100 linear classifiers (logistic regression) on a randomly sampled subset (30%) of training instances. When the training of each classifier converges, we use it to make predictions for the remaining 70% instances and record their predictions. At the end of each iteration, we compute the average prediction accuracy for each instance by calculating the ratio of correct predictions over all classifiers, and filter out instances that have a prediction accuracy ≥ 0.75 and repeat the process with

Algorithm 2: JSD based bias identification

```

Input :dataset  $\mathcal{D} = (\mathbf{X}, \mathbf{y})$ ,  $n$ -gram size  $n$ , cutoff size  $k$ 
Output:biased tokens set  $\mathcal{S}$ 
1 Initialize  $n$ -grams set  $S_{ngrams} \leftarrow \emptyset$ ;
2 Initialize positive entity distribution  $P_{positive} \leftarrow \emptyset$ ;
3 Initialize negative entity distribution  $P_{negative} \leftarrow \emptyset$ ;
4 Initialize JSD values  $Q \leftarrow \emptyset$ ;
5 foreach  $x \in \mathbf{X}$  do
6    $ngrams \leftarrow \text{FindNgrams}(x, n)$ ;
7   foreach element  $e$  of the  $ngrams$  do Add  $e$  to  $S_{ngrams}$ ;
8 end
9 foreach  $(x, y) \in (\mathbf{X}, \mathbf{y})$  do
10  foreach  $e \in ngrams$  do
11    if  $e \in x$  then Add  $(e, y)$  to  $P_{positive}$ ;
12    else Add  $(e, y)$  to  $P_{negative}$ ;
13  end
14 end
15 foreach  $e \in S_{ngrams}$  do
16   Calculate JSD values  $v$  for  $e$  using  $P_{positive}$ ,  $P_{negative}$ 
   with Equation 5.1.3;
17   Add  $(e, v)$  to  $Q$ ;
18 end
19 Select the top- $k$  elements  $\mathcal{F}$  of  $Q$  and Add  $\mathcal{F}(e)$  to  $\mathcal{S}$ ;
20 return  $\mathcal{S}$ 

```

the remaining instances for the next iteration. The algorithm terminates when less than 500 instances are filtered during one iteration or when it has reached 100 iterations. After the filtering process, any instances that are not filtered are used for to *further* fine-tune the entity predictor (BERT). Note that we apply this fine-tuning on the best model (based on validation) from contrastive learning (Section 5.1), and following previous studies [5, 22, 41] we freeze the BERT parameters and initialise (randomly) a new linear layer.

6 EXPERIMENTS

To verify the effectiveness of our proposed debiasing approach, we conduct a comprehensive study comparing our model against a number of benchmark systems. Our experiments include cross-domain/dataset generalization test, adversarial samples (created by distorting words and sentences), and utterances featuring unseen n -grams.

6.1 Datasets and Metrics

We use MultiWOZ [10] as the main dialogue dataset for our experiments. Specifically, we use version 2.2 of the dataset [50] which fixes a number of annotation errors and disallows slots with a large number of values to improve data quality. For evaluation metrics, we use the same BLEU and Entity F1 measures that we used in our preliminary investigation (Section 3).

6.2 Baselines

We compare our model against the following state-of-the-art benchmark systems:

- Mem2Seq [27]: employs a recurrent network-based decoder to generate system responses and utilize memory networks to store the KB and copy KB entities from memory via pointer mechanism. The decoder are jointly trained with memory networks end-to-end by maximizing the likelihood of the final system responses.
- GLMP [47]: employs a global-to-local pointer mechanism over the standard memory networks architecture for improving KB retrieval accuracy during response generation. The global pointer is supervised by additional training signals extracted from the standard system responses.
- DF-Net [36]: utilizes a shared-private architecture to capture both domain-specific and domain-general knowledge to improve the model transferability.
- SimpleTOD [19]: a causal language model based on GPT-2 trained on several task-oriented dialogue sub-tasks including dialogue state tracking, action prediction and response generation. It exploits additional training signals such as dialogue states and system acts compared to other systems.

6.3 Implementation Details

For delexicalized response generation, we use pretrained gpt2.⁴ We use the default hyper-parameter configuration, except for learning rate and batch size where we optimise via grid search. The learning rate is selected from $\{1e^{-3}, 1e^{-4}, 1e^{-5}, 2e^{-4}, 2e^{-4}, 2e^{-4}\}$ and batch size from $\{2, 4, 8, 16, 32\}$ based on the best validation performance.

For entity prediction, we use pretrained bert-base-uncased.⁵ During contrastive pre-training stage, the learning rate is selected from $\{1e^{-3}, 1e^{-4}, 1e^{-5}, 1e^{-6}\}$ and batch size from $\{2, 4, 8, 16, 32\}$ using grid search based on validation performance. We pre-train BERT with contrastive learning for 20 epochs. The model with the best validation performance (minimum loss) is used for fine-tuning for entity prediction. During fine-tuning stage, the learning rate is selected from $\{1e^{-3}, 1e^{-4}, 1e^{-5}, 2e^{-4}, 2e^{-4}, 2e^{-4}\}$ and the batch size from $\{2, 4, 8, 16, 32\}$. We use Adam [23] as the optimizer. In terms of n -gram order, $n = 3$ (trigram).

We run all experiments five times using different random seeds and report the average and standard deviation. All the models are trained on a single GeForce RTX 2080 Ti GPU and the training of both components (response generator and entity predictor) takes approximately one day.

6.4 Adversarial Attack Results

Language variety is one of the key features of human languages [12], i.e., we tend to express the same meaning using different words. In real-world situations, users may use very different expressions than those in the training data. To test model robustness under such situations, we perform several perturbations on user utterances in the original test set to construct adversarial test examples. We use the widely-used NlpAug library [26] to augment the “regular” user utterances to generate four adversarial test sets through: word paraphrasing (WP), word deletion (WD), sentence paraphrasing (SP), and sentence insertion (SI). All the hyper-parameters of the augmentation tool NlpAug are kept to their default. We train all

⁴<https://huggingface.co/gpt2>.

⁵<https://huggingface.co/bert-base-uncased>.

Model	Original		WP		WD		SP		SI	
	F1	BLEU	F1	BLEU	F1	BLEU	F1	BLEU	F1	BLEU
Mem2Seq [27]	23.42	4.53	7.69	3.94	8.20	3.91	9.65	4.17	10.25	4.06
GLMP [47]	33.79	6.22	10.21	5.34	10.97	5.29	13.14	5.69	14.04	5.53
DF-Net [36]	35.73	7.01	11.02	6.08	11.73	6.03	14.01	6.45	14.96	6.28
SimpleTOD [19]	35.80	20.20	11.19	9.25	12.02	9.19	14.37	10.63	15.35	10.45
Ours (w/o CL, w/ MLM) [◊]	36.74	21.05	11.33	10.99	12.67	10.97	15.01	11.53	16.47	12.24
Ours (w/ CL, Frequent n -grams) [♣]	32.20	20.61	27.85	17.87	26.66	17.23	26.44	16.33	19.90	16.04
Ours (w/ CL, Mutual Information) [♣]	31.86	20.04	28.84	18.38	26.98	17.36	27.14	16.60	23.60	16.89
Ours (w/ CL, Jensen-Shannon Divergence) [♣]	31.50	19.42	29.15	18.96	28.13	18.33	28.95	17.81	23.96	17.37
Ours (w/o CL, w/ AF) [◊]	31.35	20.37	27.22	17.80	26.51	17.57	26.04	17.14	21.30	16.49
Ours (w/ CL, w/ AF) [◊]	30.98	19.26	29.89	19.01	29.28	18.93	29.20	18.06	28.69	17.59

Table 2: Adversarial attack results. All the models are trained on the original (unperturbed) MultiWOZ data using all domains. “Original” denote the original MultiWOZ test set, while “WP”, “WD”, “SP” and “SI” denote adversarial test sets created through word paraphrasing, word deletion, sentence paraphrasing and sentence insertion respectively, using NlpAug [26]. \diamond : Our vanilla model without contrastive learning or adversarial filtering; \clubsuit : our model with contrastive learning; \heartsuit : our model with adversarial filtering.

Model	All F1	All BLEU	Restaurant F1	Hotel F1	Attraction F1	Training F1
	10.38 (± 0.28)	4.27 (± 0.79)	13.51 (± 0.13)	5.59 (± 0.26)	14.85 (± 0.30)	8.66 (± 0.50)
Mem2Seq [27]	14.25 (± 0.20)	5.84 (± 0.05)	18.93 (± 0.42)	7.06 (± 0.47)	20.95 (± 0.29)	11.67 (± 0.20)
GLMP [47]	15.17 (± 0.31)	6.61 (± 0.41)	20.10 (± 0.20)	7.61 (± 0.30)	22.23 (± 0.43)	12.46 (± 0.29)
DF-Net [36]	15.57 (± 0.17)	12.79 (± 0.25)	20.64 (± 0.12)	7.78 (± 0.10)	22.83 (± 0.30)	12.78 (± 0.14)
SimpleTOD [19]	15.82 (± 0.46)	14.36 (± 0.21)	18.04 (± 0.09)	8.68 (± 0.11)	23.16 (± 0.19)	14.49 (± 0.47)
Ours (w/o CL, w/ MLM) [◊]	20.33 (± 0.15)	17.17 (± 0.15)	22.29 (± 0.09)	10.23 (± 0.21)	20.82 (± 0.12)	9.65 (± 0.02)
Ours (w/ CL, Mutual Information) [♣]	21.25 (± 0.04)	17.86 (± 0.05)	20.80 (± 0.05)	12.91 (± 0.31)	26.05 (± 0.28)	13.72 (± 0.16)
Ours (w/ CL, Jensen-Shannon Divergence) [♣]	26.42 (± 0.14)	21.83 (± 0.07)	28.46 (± 0.15)	14.72 (± 0.07)	27.07 (± 0.12)	15.64 (± 0.04)
Ours (w/o CL, w/ AF) [◊]	20.26 (± 0.11)	15.53 (± 0.25)	20.30 (± 0.08)	10.04 (± 0.06)	24.31 (± 0.04)	14.22 (± 0.19)
Ours (w/ CL, w/ AF) [◊]	29.80 (± 0.27)	22.05 (± 0.15)	27.51 (± 0.37)	22.59 (± 0.17)	40.07 (± 0.09)	15.72 (± 0.28)

Table 3: Unseen utterances generalization test results. All the training and inference are done on the new train/test splits (see Section 6.5) created to reduce n -gram overlap between training and test data. “F1 (All)”: testing F1 using all the domains; “BLEU (All)”: testing BLEU using all the domains; “Training F1”: F1 results on training partition using all the domains. We run each experiment five times with different random seeds and report the average results with standard deviation (in parenthesis).

systems (benchmark and ours) using the *original* MultiWOZ and test them on both the original test set and adversarial test sets. Results are shown in Table 2⁶.

Our model has several variants: (1) vanilla without any debiasing, noting that it still has domain adaptive pre-training using the masked language model loss (\diamond); (2) with contrastive loss for domain-adaptive pre-training (\clubsuit); and (3) with adversarial filtering, applied with or without contrastive pre-training (\heartsuit). The reason why our vanilla model has masked language model pre-training is that we need to understand that when we introduce contrastive pre-training, any performance gain is attributed to the contrastive learning objective rather than the domain adaptive pre-training step.

Looking at the original test set (“Original”), among the benchmark systems SimpleTOD is the best model, and our vanilla model

(\diamond) performs similarly (marginally better F1 but lower BLEU). Introducing contrastive learning (\clubsuit) and adversarial filtering (\heartsuit) somewhat degrades the entity prediction performance (F1), although the quality of the generated response (BLEU) is less impacted. Moving on to the adversarial test sets, all benchmark systems and our vanilla model observe severe performance degradation: F1 drops by over 20 points and BLEU by 10 points for most systems, suggesting that these models are not robust against perturbed inputs. Our systems with contrastive learning and/or adversarial filtering, on the other hand, look promising: the drop is substantially less severe, 2-3 points in terms of F1 and BLEU. Interestingly, we also see that SI appears to be the most challenging test set as its performance is lowest. Comparing the three different criteria for ranking n -grams (frequent n -gram, mutual information and Jensen-Shannon divergence), Jensen-Shannon divergence appears to have the upper hand, suggesting that label information and both the presence and absence of an n -gram is important for uncovering shortcuts in the data.

⁶Due to space limit, we report average performance for adversarial attack experiment. For other experiments, we report both average and standard deviation.

Model	Hotel,Attraction,Train → Restaurant		Restaurant,Attraction,Train → Hotel		Restaurant,Hotel,Train → Attraction		Restaurant,Hotel,Attraction → Train	
	F1	BLEU	F1	BLEU	F1	BLEU	F1	BLEU
Mem2Seq [27]	9.70 (±0.04)	4.88 (±0.56)	2.87 (±0.30)	3.89 (±0.48)	6.97 (±0.16)	3.67 (±0.66)	2.89 (±0.08)	3.03 (±0.05)
GLMP [47]	13.22 (±0.36)	6.75 (±0.09)	2.98 (±0.47)	5.26 (±0.51)	9.13 (±0.40)	4.94 (±0.11)	3.00 (±0.19)	3.98 (±0.26)
DF-Net [36]	14.09 (±0.69)	7.57 (±0.04)	3.32 (±0.38)	5.99 (±0.49)	9.79 (±0.58)	5.66 (±0.10)	3.34 (±0.24)	4.65 (±0.52)
SimpleTOD [19]	14.46 (±0.47)	13.78 (±0.40)	3.36 (±0.08)	11.16 (±0.27)	10.03 (±0.15)	11.82 (±0.09)	3.38 (±0.45)	13.77 (±0.39)
Ours (w/o CL, w/ MLM)◊	14.95 (±0.35)	14.23 (±0.07)	5.80 (±0.02)	13.81 (±0.11)	10.31 (±0.19)	12.93 (±0.42)	3.77 (±0.34)	14.91 (±0.03)
Ours (w/ CL, Frequent n -grams)♣	19.09 (±0.20)	15.27 (±0.07)	12.34 (±0.27)	14.56 (±0.09)	13.62 (±0.14)	14.32 (±0.26)	10.25 (±0.41)	14.93 (±0.06)
Ours (w/ CL, Mutual Information)♣	22.24 (±0.19)	15.33 (±0.26)	14.85 (±0.35)	14.60 (±0.14)	15.05 (±0.26)	15.93 (±0.44)	11.76 (±0.08)	17.46 (±0.47)
Ours (w/ CL, Jensen-Shannon Divergence)♣	23.14 (±0.25)	15.68 (±0.13)	18.01 (±0.38)	15.01 (±0.25)	19.61 (±0.47)	16.38 (±0.07)	12.48 (±0.32)	18.86 (±0.44)
Ours (w/o CL, w/ AF)◊	21.30 (±0.17)	16.35 (±0.14)	15.26 (±0.33)	14.96 (±0.48)	16.76 (±0.41)	16.12 (±0.18)	10.86 (±0.31)	16.30 (±0.11)
Ours (w/ CL, w/ AF)◊	25.13 (±0.29)	17.93 (±0.35)	23.86 (±0.17)	15.83 (±0.12)	21.37 (±0.20)	16.90 (±0.09)	14.43 (±0.13)	19.03 (±0.08)

Table 4: Cross-domain generalization results. “X→Y”: X denote the training domain(s) and Y the test domain.

Model	MultiWOZ→SMD		MultiWOZ→SGD	
	F1	BLEU	F1	BLEU
Mem2Seq [27]	9.06 (±0.49)	8.01 (±0.33)	4.34 (±0.28)	3.48 (±0.63)
GLMP [47]	12.25 (±0.21)	11.45 (±0.74)	5.18 (±0.47)	4.66 (±0.38)
DF-Net [36]	13.07 (±0.71)	12.51 (±0.57)	5.63 (±0.79)	5.36 (±0.94)
SimpleTOD [19]	13.41 (±0.41)	13.87 (±0.37)	5.75 (±0.81)	7.51 (±0.29)
Ours (w/o CL, w/ MLM)♣	13.57 (±0.44)	14.45 (±0.69)	6.06 (±0.77)	8.94 (±0.76)
Ours (w/ CL, Frequent n -grams)♣	19.01 (±0.70)	15.25 (±0.44)	9.44 (±0.78)	10.07 (±0.73)
Ours (w/ CL, Mutual Information)♣	20.32 (±0.42)	15.44 (±0.15)	9.79 (±0.81)	10.38 (±0.76)
Ours (w/ CL, Jensen-Shannon Divergence)♣	21.80 (±0.68)	15.70 (±0.67)	11.23 (±0.14)	10.68 (±0.07)
Ours (w/o CL, w/ AF)◊	20.44 (±0.39)	15.43 (±0.62)	9.73 (±0.04)	10.25 (±0.11)
Ours (w/ CL, w/ AF)◊	23.79 (±0.49)	18.25 (±0.23)	11.41 (±0.21)	10.99 (±0.05)

Table 5: Cross-dataset generalization results. “A→B”: a model is trained using train partition of dataset A and evaluated on the test partition of dataset B in a zero-shot manner.

6.5 Unseen Utterances Generalization Results

To test our model’s generalization capability under unseen scenario, we construct a new MultiWOZ split that aims to reduce n -gram overlap between training and test data. We first collect all n -gram types in the full data (training + test) and remove low frequency (< 10) n -grams, and then create two sets of n -grams based on their frequencies: “train” which contains the most frequent (70%) n -gram types and “test” for the remaining (30%). These two sets will decide whether an instance will be assigned to the training or test partition. That is, we iterate each instance from the full data and put it to the training partition if it only contains “train” n -gram, or the test partition if it has only “test” n -gram.⁷

Empirically, in the original MultiWOZ split the n -gram overlap ratio is 82.75%; our new split reduces this to 51.2%. This means that during testing, a model using our split will be exposed to utterances with more unseen phrases, and if the model exploits the spurious cues (n -grams) in the input it will likely to perform poorly under this new split, as these cues are more likely to be absent.

⁷For instances containing both “train” n -grams and “test” n -grams, we put them to the training partition or test partition according to the majority type. If the numbers of “train” n -grams and “test” n -grams are equal for an instance, we put it to the training partition.

We train all models using the new training partition and test them on the new test partition and present the results in Table 3. Looking at the models without debiasing, we find a similar observation where SimpleTOD and our vanilla model (◊) are the best performing models over different domains. When we introduce contrastive learning (♣) and adversarial filtering (◊), we see an improvement over all domains, with the best variant that combines both (“w/ CL, w/ AF”) improving over the vanilla model by a large margin, about 14% in Entity F1 and 8% in BLEU. As before, using Jensen-Shannon divergence as the criterion for ranking n -grams turns out to be the best approach. Contrastive learning and adversarial filtering seem to provide complementary signal based on this experiment, as combining them both produces substantially better performance.

To understand how these two methods complement each other, we present F1 performance in the training partition (last column in Table 3): here we see that the models that are not debiased have similar training and test performance, while the contrastive models (♣) have a much lower training performance, suggesting there is underfitting. Adversarial filtering, however, does not suffer from this problem (“w/o CL, w/ AF”), as it only removes training instances that do not negatively impact training accuracy. Interestingly, when

we incorporate adversarial filtering to the contrastive model (“w/ CL, w/ AF”), this underfitting problem is corrected, showing their complementarity.

6.6 Cross-domain Generalization Results

We now test cross-domain generalization, where a model is tested using a domain that is not in the training data.

We use the “leave-one-out” strategy for this, where a model is trained using all except one domain and tested using that unseen domain. We present the results in Table 4.

We see similar observations here. Without any debiasing, SimpleTOD and our vanilla have the best performances. When we incorporate contrastive learning and adversarial filtering, we see a strong improvement in terms of model robustness. As before, the best variant is one that combines both, and when compared to the vanilla model it improves F1 by 10–18 and BLEU by 2–5 points depending on the test domain. For contrastive learning, Jensen-Shanon divergence is again the best criterion for selecting n -grams. Adversarial filtering by itself is also fairly effective, although not as effective as the best contrastive model.

6.7 Cross-dataset Results

We now test the hardest setting: cross-dataset generalization. If a model “overfits” a dataset and relies on spurious correlations to perform a task, it will likely to perform very poorly in a new dataset of the same task. In this experiment, we train systems on MultiWOZ, and test them on two other popular datasets for task-oriented dialogues: SMD [11] and SGD [38]. For SGD, it doesn’t have a database like SMD and MultiWOZ. Following [38], we collect the returned entities from the API queries during each dialogue as the database records to mimic the data settings of SMD and MultiWOZ.

The results are shown in Table 5. Both contrastive learning and adversarial filtering are effective methods to improve model robustness. The best contrastive model (“w/ Jensen-Shanon divergence”) improves F1 by 5–8 and BLEU by 1–2 points when compared to the vanilla model. Adversarial filtering by itself is also effective, although the improvement is marginally smaller compared to the best contrastive model. Once again, combining both produces the best performance. SGD is noticeably a harder dataset here, where F1 performance of all models is about half of SMD’s.

All in all these generalization tests reveal strikingly similar observations. To summarize: (1) our vanilla model that decomposes task-oriented dialogue generation into delexicalized response generation and entity prediction performs competitively with benchmark systems; (2) for contrastive learning, Jensen-Shanon divergence is consistently the best performer for ranking n -grams, implying that it is important to consider both the absence and presence of n -grams when determining their correlations with the labels; and (3) contrastive learning and adversarial filtering complement each other, and the most robust model is produced by incorporating both methods. Note that although our experiments focus on task-oriented dialogue, our methodology can be adapted to other NLP tasks without much difficulty. We believe that our contrastive pre-training method is likely useful to reduce general NLP data

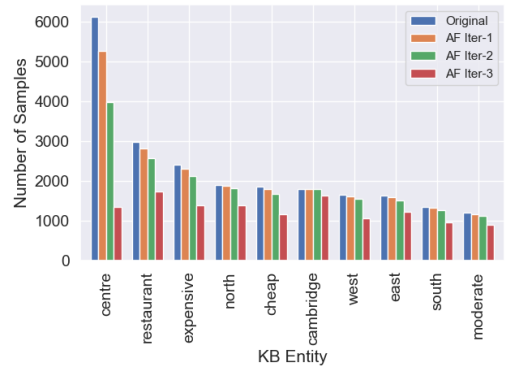


Figure 3: Change in entity frequency over different iterations of adversarial filtering. X-axis shows the 10 most frequent entity labels in the response. Y-axis shows the frequency of training instances for an entity. “Original”: Entity frequency without any filtering; “AF Iter- k ”: Entity frequency after k iterations of filtering.

artifacts, as spurious correlations between words and labels are likely to surface during data development.

6.8 Adversarial Filtering Dynamics Analysis

The adversarial filtering iteratively detects the easy training instances and remove them. A natural question to ask is: why does this filtering process make the model more robust? To answer this question, we perform an analysis on the dynamics of the iterative process where we analyzed the number of instances containing a particular entity. We select the top-10 most frequent entities in the response and monitor their change in frequency over the iterations and present the results in Figure 3. As we can see from the figure, the distribution over these 10 entities has become “flatter” after the third iteration (red bars). The more frequent an entity is, the more instances are removed: at the extreme, the most frequent entity (*centre*) has lost almost 5000 instances after 3 iterations of filtering. Intuitively, we believe the more balanced distribution disincentivizes the model to focus on shortcuts that produce the frequent labels (entities), resulting in a model that learns generalisable patterns from a larger set of entities in the tail of the distribution.

7 CONCLUSION

In this work, we investigate data artifacts in MultiWOZ, a popular task-oriented dialogue dataset. We find that a model that uses full input for training performs similarly to a variant that uses partial input containing only frequent phrases, suggesting that there are data artifacts and the model uses them as shortcuts for the task. Motivated by this analysis, we propose a contrastive learning objective to debias task-oriented dialogue models by encouraging models to ignore these frequent phrases to focus on semantic words in the input. We also adapt adversarial filtering to our task to further improve model robustness. We conduct a series of generalization experiments, testing our method and a number of state-of-the-art benchmarks. Experimental results show that contrastive learning and adversarial filtering complement each other, and combining both produces the most robust dialogue model.

REFERENCES

- [1] Yonatan Belinkov, Adam Poliak, Stuart M. Shieber, Benjamin Van Durme, and Alexander M. Rush. 2019. Don't Take the Premise for Granted: Mitigating Artifacts in Natural Language Inference. *arXiv:1907.04380* [cs.CL]
- [2] Antoine Bordes, Y-Lan Boureau, and Jason Weston. 2017. Learning End-to-End Goal-Oriented Dialog.. In *ICLR*. <http://dblp.uni-trier.de/db/conf/iclr/iclr2017.html#BordesBW17>
- [3] Ruben Branco, António Branco, João António Rodrigues, and João Ricardo Silva. 2021. Shortcuted Commonsense: Data Spuriousness in Deep Learning of Commonsense Reasoning. In *Proceedings of the 2021 Conference on Empirical Methods in Natural Language Processing*. Association for Computational Linguistics, Online and Punta Cana, Dominican Republic, 1504–1521. <https://doi.org/10.18653/v1/2021.emnlp-main.113>
- [4] Paweł Budzianowski, Tsung-Hsien Wen, Bo-Hsiang Tseng, Iñigo Casanueva, Stefan Ultes, Osman Ramadan, and Milica Gasic. 2018. MultiWOZ-A Large-Scale Multi-Domain Wizard-of-Oz Dataset for Task-Oriented Dialogue Modelling. In *Proceedings of the 2018 Conference on Empirical Methods in Natural Language Processing*. 5016–5026.
- [5] Ting Chen, Simon Kornblith, Mohammad Norouzi, and Geoffrey Hinton. 2020. A Simple Framework for Contrastive Learning of Visual Representations. *arXiv:2002.05709* [cs.LG]
- [6] Wenhui Chen, Jianshu Chen, Pengda Qin, Xifeng Yan, and William Yang Wang. 2019. Semantically Conditioned Dialog Response Generation via Hierarchical Disentangled Self-Attention. In *Proceedings of the 57th Annual Meeting of the Association for Computational Linguistics*. 3696–3709. <https://doi.org/10.18653/v1/P19-1360>
- [7] Yun-Nung Chen, Dilek Hakkani-Tür, Gökhan Tür, Jianfeng Gao, and Li Deng. 2016. End-to-end memory networks with knowledge carryover for multi-turn spoken language understanding.. In *Interspeech*. 3245–3249.
- [8] Jacob Devlin, Ming-Wei Chang, Kenton Lee, and Kristina Toutanova. 2018. Bert: Pre-training of deep bidirectional transformers for language understanding. *arXiv preprint arXiv:1810.04805* (2018).
- [9] Jacob Devlin, Ming-Wei Chang, Kenton Lee, and Kristina Toutanova. 2019. BERT: Pre-training of Deep Bidirectional Transformers for Language Understanding. In *Proceedings of the 2019 Conference of the North American Chapter of the Association for Computational Linguistics: Human Language Technologies, Volume 1 (Long and Short Papers)*. 4171–4186.
- [10] Mihai Eric, Rahul Goel, Shachi Paul, Abhishek Sethi, Sanchit Agarwal, Shuyag Gao, and Dilek Hakkani-Tür. 2019. Multiwoz 2.1: Multi-domain dialogue state corrections and state tracking baselines. *arXiv preprint arXiv:1907.01669* (2019).
- [11] Mihai Eric, Lakshmi Krishnan, Francois Charette, and Christopher D. Manning. 2017. Key-Value Retrieval Networks for Task-Oriented Dialogue. In *Proceedings of the 18th Annual SIGdial Meeting on Discourse and Dialogue*. 37–49. <https://www.aclweb.org/anthology/W17-5506>
- [12] Jatin Ganhotra, Robert Moore, Sachindra Joshi, and Kahini Wadhawan. 2020. Effects of Naturalistic Variation in Goal-Oriented Dialog. *arXiv:2010.02260* [cs.CL]
- [13] Tianyu Gao, Xingcheng Yao, and Danqi Chen. 2021. SimCSE: Simple Contrastive Learning of Sentence Embeddings. *arXiv:2104.08821* [cs.CL]
- [14] Mor Geva, Yoav Goldberg, and Jonathan Berant. 2019. Are We Modeling the Task or the Annotator? An Investigation of Annotator Bias in Natural Language Understanding Datasets. *arXiv:1908.07898* [cs.CL]
- [15] Marjan Ghazvininejad, Chris Brockett, Ming-Wei Chang, Bill Dolan, Jianfeng Gao, Wen-tau Yih, and Michel Galley. 2018. A knowledge-grounded neural conversation model. In *Thirty-Second AAAI Conference on Artificial Intelligence*.
- [16] Suchin Gururangan, Ana Marasović, Swabha Swayamdipta, Kyle Lo, Iz Beltagy, Doug Downey, and Noah A. Smith. 2020. Don't Stop Pretraining: Adapt Language Models to Domains and Tasks. In *Proceedings of the 58th Annual Meeting of the Association for Computational Linguistics*. Online, 8342–8360.
- [17] He He, Sheng Zha, and Haohan Wang. 2019. Unlearn Dataset Bias in Natural Language Inference by Fitting the Residual. *arXiv:1908.10763* [cs.CL]
- [18] Dan Hendrycks, Kevin Zhao, Steven Basart, Jacob Steinhardt, and Dawn Song. 2021. Natural Adversarial Examples. *arXiv:1907.07174* [cs.LG]
- [19] Ehsan Hosseini-Asl, Bryan McCann, Chien-Sheng Wu, Semih Yavuz, and Richard Socher. 2020. A simple language model for task-oriented dialogue. *arXiv preprint arXiv:2005.00796* (2020).
- [20] Xiao Huang, Jingyuan Zhang, Dingcheng Li, and Ping Li. 2019. Knowledge graph embedding based question answering. In *Proceedings of the Twelfth ACM International Conference on Web Search and Data Mining*. ACM, 105–113.
- [21] Andrew Ilyas, Shibani Santurkar, Dimitris Tsipras, Logan Engstrom, Brandon Tran, and Aleksander Madry. 2019. Adversarial Examples Are Not Bugs, They Are Features. *arXiv:1905.02175* [stat.ML]
- [22] Prannay Khosla, Piotr Teterwak, Chen Wang, Aaron Sarna, Yonglong Tian, Phillip Isola, Aaron Maschinot, Ce Liu, and Dilip Krishnan. 2021. Supervised Contrastive Learning. *arXiv:2004.11362* [cs.LG]
- [23] Diederik P Kingma and Jimmy Ba. 2014. Adam: A method for stochastic optimization. *arXiv preprint arXiv:1412.6980* (2014).
- [24] Wenqiang Lei, Xisen Jin, Min-Yen Kan, Zhaochun Ren, Xiangnan He, and Dawei Yin. 2018. Seqicity: Simplifying Task-oriented Dialogue Systems with Single Sequence-to-Sequence Architectures. In *Proceedings of the 56th Annual Meeting of the Association for Computational Linguistics*.
- [25] Jiexi Liu, Ryuichi Takanobu, Jiaxin Wen, Dazhen Wan, Hongguang Li, Weiran Nie, Cheng Li, Wei Peng, and Minlie Huang. 2021. Robustness Testing of Language Understanding in Task-Oriented Dialog. *arXiv:2012.15262* [cs.CL]
- [26] Edward Ma. 2019. NLP Augmentation. <https://github.com/makcedward/nlpaug>.
- [27] Andrea Madotto, Chien-Sheng Wu, and Pascale Fung. 2018. Mem2Seq: Effectively Incorporating Knowledge Bases into End-to-End Task-Oriented Dialog Systems. In *Proceedings of the 56th Annual Meeting of the Association for Computational Linguistics (Volume 1: Long Papers)*. 1468–1478. <https://www.aclweb.org/anthology/P18-1136>
- [28] R. Thomas McCoy, Ellie Pavlick, and Tal Linzen. 2019. Right for the Wrong Reasons: Diagnosing Syntactic Heuristics in Natural Language Inference. *arXiv:1902.01007* [cs.CL]
- [29] Yulei Niu, Kaihua Tang, Hanwang Zhang, Zhiwu Lu, Xian-Sheng Hua, and Ji-Rong Wen. 2021. Counterfactual VQA: A Cause-Effect Look at Language Bias. *arXiv:2006.04315* [cs.CV]
- [30] Timothy Niven and Hung-Yu Kao. 2019. Probing Neural Network Comprehension of Natural Language Arguments. *arXiv:1907.07355* [cs.CL]
- [31] Kishore Papineni, Salim Roukos, Todd Ward, and Wei-Jing Zhu. 2002. BLEU: a method for automatic evaluation of machine translation. In *Proceedings of the 40th annual meeting on association for computational linguistics*.
- [32] Baolin Peng, Chunyuan Li, Jinchao Li, Shahin Shayandeh, Lars Liden, and Jianfeng Gao. 2020. SOLOIST: Building Task Bots at Scale with Transfer Learning and Machine Teaching. *arXiv preprint arXiv:2005.05298* (2020).
- [33] Baolin Peng, Chunyuan Li, Zhu Zhang, Chenguang Zhu, Jinchao Li, and Jianfeng Gao. 2020. RADDLE: An Evaluation Benchmark and Analysis Platform for Robust Task-oriented Dialog Systems. *arXiv:2012.14666* [cs.CL]
- [34] Baolin Peng, Xiuju Li, Jianfeng Gao, Jingjing Liu, and Kam-Fai Wong. 2018. Deep Dyna-Q: Integrating Planning for Task-Completion Dialogue Policy Learning. In *Proceedings of the 56th Annual Meeting of the Association for Computational Linguistics (Volume 1: Long Papers)*. 2182–2192.
- [35] Jiaxin Qi, Yulei Niu, Jianqiang Huang, and Hanwang Zhang. 2020. Two Causal Principles for Improving Visual Dialog. *arXiv:1911.10496* [cs.CV]
- [36] Libo Qin, Xiao Xu, Wanxiang Che, Yue Zhang, and Ting Liu. 2020. Dynamic Fusion Network for Multi-Domain End-to-end Task-Oriented Dialog. In *Proceedings of the 58th Annual Meeting of the Association for Computational Linguistics*. Association for Computational Linguistics, Online, 6344–6354. <https://www.aclweb.org/anthology/2020.acl-main.565>
- [37] Alec Radford, Jeffrey Wu, Rewon Child, David Luan, Dario Amodei, Ilya Sutskever, et al. 2019. Language models are unsupervised multitask learners. *OpenAI blog* 1, 8 (2019), 9.
- [38] Abhinav Rastogi, Xiaoxue Zang, Srinivas Sunkara, Raghav Gupta, and Pranav Khaitan. 2020. Towards Scalable Multi-domain Conversational Agents: The Schema-Guided Dialogue Dataset. *arXiv:1909.05855* [cs.CL]
- [39] Keisuke Sakaguchi, Ronan Le Bras, Chandra Bhagavatula, and Yejin Choi. 2019. WinoGrande: An Adversarial Winograd Schema Challenge at Scale. *arXiv:1907.10641* [cs.CL]
- [40] Victor Sanh, Thomas Wolf, Yonatan Belinkov, and Alexander M. Rush. 2020. Learning from others' mistakes: Avoiding dataset biases without modeling them. *arXiv:2012.01300* [cs.CL]
- [41] Yonglong Tian, Dilip Krishnan, and Phillip Isola. 2020. Contrastive Multiview Coding. *arXiv:1906.05849* [cs.CV]
- [42] Aaron van den Oord, Yazhe Li, and Oriol Vinyals. 2019. Representation Learning with Contrastive Predictive Coding. *arXiv:1807.03748* [cs.LG]
- [43] Petar Veličković, Guillem Cucurull, Arantxa Casanova, Adriana Romero, Pietro Lio, and Yoshua Bengio. 2017. Graph attention networks. *arXiv preprint arXiv:1710.10903* (2017).
- [44] Thomas Wolf, Victor Sanh, Julien Chaumond, and Clement Delangue. 2019. Transfertransfo: A transfer learning approach for neural network based conversational agents. *arXiv preprint arXiv:1901.08149* (2019).
- [45] Chien-Sheng Wu, Steven Hoi, Richard Socher, and Caiming Xiong. 2020. TOD-BERT: pre-trained natural language understanding for task-oriented dialogue. *arXiv preprint arXiv:2004.06871* (2020).
- [46] Chien-Sheng Wu, Andrea Madotto, Ehsan Hosseini-Asl, Caiming Xiong, Richard Socher, and Pascale Fung. 2019. Transferable Multi-Domain State Generator for Task-Oriented Dialogue Systems. *arXiv preprint arXiv:1905.08743* (2019).
- [47] Chien-Sheng Wu, Richard Socher, and Caiming Xiong. 2019. Global-to-local Memory Pointer Networks for Task-Oriented Dialogue.. In *ICLR*. <http://dblp.uni-trier.de/db/conf/iclr/iclr2019.html#WuSX19>
- [48] Qi Wu, Peng Wang, Chunhua Shen, Anthony Dick, and Anton Van Den Hengel. 2016. Ask me anything: Free-form visual question answering based on knowledge from external sources. In *Proceedings of the IEEE conference on computer vision and pattern recognition*.
- [49] Chen Xing, Yu Wu, Wei Wu, Yalou Huang, and Ming Zhou. 2018. Hierarchical recurrent attention network for response generation. In *Thirty-Second AAAI*

Conference on Artificial Intelligence.

- [50] Xiaoxue Zang, Abhinav Rastogi, Srinivas Sunkara, Raghav Gupta, Jianguo Zhang, and Jindong Chen. 2020. MultiWOZ 2.2 : A Dialogue Dataset with Additional Annotation Corrections and State Tracking Baselines. *arXiv:2007.12720 [cs.CL]*
- [51] Yichi Zhang, Zhijian Ou, and Zhou Yu. 2020. Task-oriented dialog systems that consider multiple appropriate responses under the same context. In *Proceedings of the AAAI Conference on Artificial Intelligence*, Vol. 34. 9604–9611.
- [52] Yizhe Zhang, Siqi Sun, Michel Galley, Yen-Chun Chen, Chris Brockett, Xiang Gao, Jianfeng Gao, Jingjing Liu, and Bill Dolan. 2019. Dialogpt: Large-scale generative pre-training for conversational response generation. *arXiv preprint arXiv:1911.00536* (2019).
- [53] Victor Zhong, Caiming Xiong, and Richard Socher. 2018. Global-locally self-attentive dialogue state tracker. *arXiv preprint arXiv:1805.09655* (2018).